https://doi.org/10.5194/egusphere-2026-4409
Preprint. Discussion started: 30 July 2026
© Author(s) 2026. CC BY 4.0 License.

An Expanded Methanosphere: Methane Oxidation and Methanotrophs Surrounding Cold Seeps Across Oxygen Gradients on the Southern California Margin

Emily Klonicki-Ference[1*], Daniel R. Utter[2], Kira Homola[1], John S. Magyar[2], Victoria J. Orphan[2], David W. Caress[3], Jennifer B. Paduan[3], Lisa Levin[4], Tina Treude[1,5*]

[1]Department of Earth, Planetary, and Space Sciences, University of California Los Angeles, Los Angeles, CA, USA

[2]Division of Geological and Planetary Sciences, California Institute of Technology, Pasadena, CA,
USA

[3] Monterey Bay Aquarium Research Institute, 7700 Sandholdt Road, Moss Landing CA USA

[4]Scripps Institution of Oceanography, University of California, San Diego, La Jolla, CA, USA

[5]Department of Atmospheric and Oceanic Sciences, University of California Los Angeles, Los Angeles, CA, USA

*Correspondence: Tina Treude, ttreude@g.ucla.edu; Emily Klonicki-Ference, eklonicki@g.ucla.edu

Abstract

Marine methane (CH_4) seeps are dynamic biogeochemical systems that regulate carbon and sustain high-biomass communities through microbial CH_4 oxidation. While most CH_4 is consumed anaerobically in sediments, a fraction escapes into the water column, where aerobic methanotrophs act as a biological filter limiting atmospheric flux. However, the spatial extent of CH_4 influence beyond active seep zones remains poorly constrained, with implications for deep-sea food webs and carbon cycling. We investigated microbial CH_4 turnover and methanotroph distribution across three seep sites on the Southern California margin (Del Mar (1020 m), Santa Monica Mound (800 m), and Lasuen Knoll (400 m)) focusing on extent of horizontal transport, presence of vertical gradients, and oxygen controls. Using radiotracer (^3H-CH_4) incubations, CH_4 concentration profiles, 16S rRNA gene sequencing, and particulate methane monooxygenase (pmoA) gene quantification, we characterized CH_4-fueled processes along vertical and lateral transects, including near-bottom waters sampled via HOV *Alvin*. CH_4 oxidation was active both

https://doi.org/10.5194/egusphere-2026-4409
Preprint. Discussion started: 30 July 2026
© Author(s) 2026. CC BY 4.0 License.

within seep plumes and in off-seep waters extending hundreds of meters from the source, with maximum rates reaching 454 nmol L^{-1} d^{-1} in a CH_4-rich bubble plume. Methanotrophic communities showed vertical structuring, with higher diversity near the seafloor. pmoA gene abundances remained consistent across seep and seep-adjacent environments, indicating widespread oxidation potential. Environmental controls were site-specific: oxidation correlated positively with CH_4 and negatively with oxygen at some sites, whereas oxygen enhanced oxidation at others. These findings support an expanded "methanosphere," in which CH_4-driven microbial processes extend beyond seep boundaries, linking local seep activity to broader deep-sea biogeochemical dynamics.

1 Introduction

Although once regarded as rare and biologically limited, deep-sea methane (CH_4) seeps, also referred to as cold seeps, are now increasingly recognized as critical ecosystems that support the health and functioning of broader deep-sea communities (Boetius & Wenzhöfer, 2013; Levin, 2005; Levin et al., 2016; Sibuet & Roy, 2002; Thurber et al., 2014; Treude et al., 2011). Distributed widely along continental margins (Judd & Hovland, 2009), these dynamic environments may play a far more expansive ecological role than previously understood, with implications that extend beyond the boundaries of seep-specific habitats. CH_4 seeps form where CH_4 is released from subsurface sources driven by vertical fluid advection (Suess, 2010). These discharges fuel high-biomass ecosystems sustained by chemosynthesis, fundamentally altering local biodiversity and geochemistry (Levin, 2005; Paull et al., 1984; Suess, 2010; Tunnicliffe et al., 2003). Cold-seep ecosystems are structured by CH_4- and sulfide-oxidizing chemosynthetic microorganisms, along with a range of fauna that indirectly rely on CH_4-derived carbon (Levin, 2005).

Within seep sediments and associated authigenic carbonates, the anaerobic oxidation of CH_4 is tightly coupled to sulfate (SO_4^{2-}) reduction and acts as a significant biological filter, limiting the emission of CH_4 into the overlying water (Hinrichs & Boetius, 2002; Knittel & Boetius, 2009; Marlow et al., 2014; Treude et al., 2003). Sulfide generated through this process supports dense mats of sulfur-oxidizing bacteria and sustains a diverse assemblage of chemosymbiotic invertebrates, such as tubeworms and bivalves (Cavanaugh, 1983; Dubilier et al., 2008).

https://doi.org/10.5194/egusphere-2026-4409
Preprint. Discussion started: 30 July 2026
© Author(s) 2026. CC BY 4.0 License.

CH_4 that escapes this benthic CH_4 filter is oxidized aerobically by CH_4-oxidizing bacteria (MOB) in the overlying water column (Reeburgh, 2007), according to the reaction:

$$CH_4 + 2O_2 \rightarrow CO_2 + 2H_2O \qquad \text{(Eq. 1)}$$

MOB, which are phylogenetically diverse and metabolically adaptable, play a central role in mitigating CH_4 emissions from the ocean (Reeburgh, 2007). MOB occur throughout the marine water column, from well-oxygenated surface waters to low-oxygen (O_2) and even anoxic zones, depending on environmental conditions such as CH_4 availability, O_2 concentration, and particle flux (Reeburgh, 2007; Steinle et al., 2015; Tavormina et al., 2010; Thamdrup et al., 2019). These bacteria catalyze CH_4 oxidation using methane monooxygenase, the enzyme responsible for the conversion of CH_4 to methanol, the first and rate-limiting step of CH_4 oxidation. MMO exists in two forms: particulate methane monooxygenase (pMMO), a membrane-bound, copper-dependent enzyme that is widely distributed and typically expressed under high-copper conditions, and soluble methane monooxygenase (sMMO), a cytoplasmic, iron-containing enzyme that is expressed under copper-limiting conditions in some methanotrophs (Kalyuzhnaya et al., 2013; Semrau et al., 2010). Most marine MOB encode and express pMMO, which is considered the dominant form of methane monooxygenase among methanotrophs in seawater.

Beyond their free-living forms, MOB also establish symbiotic relationships with protozoan and metazoan hosts. Such symbioses are well documented in CH_4-rich settings like cold seeps and hydrothermal vents, where MOB occur as endosymbionts in bathymodiolin mussels (Childress et al., 1986), frenulate siboglinids (formerly pogonophora) (Levin, 2005), feather duster worms (Goffredi et al., 2020; Schmaljohann & Flügel, 1987), folliculinid ciliates (Pasulka et al., 2017), and sponges (Rubin-Blum et al., 2019) or as ectosymbionts in sea spiders (Dal Bó et al., 2025). In these partnerships, MOB supply CH_4-derived organic carbon to their hosts, enabling persistence in CH_4-rich environments that are depleted in photosynthetic carbon sources. Even minimal CH_4 flux from sediments to the water column supports benthic chemosynthetic processes, while methanotrophs in the overlying water oxidize CH_4 across broad spatial and vertical gradients, shaping both local and regional carbon cycles (Damm et al., 2010).

https://doi.org/10.5194/egusphere-2026-4409
Preprint. Discussion started: 30 July 2026
© Author(s) 2026. CC BY 4.0 License.

While CH_4 seeps are known for structuring benthic communities, they may also influence pelagic processes at broader spatial scales. CH_4 that surpasses the sediment-water interface fuels aerobic methanotrophy in the water column, which regulates CH_4 fluxes to the atmosphere, removes O_2, alters microbial community structure, and potentially supports pelagic food webs through the transfer of CH_4-derived carbon (Damm et al., 2010; Steinle et al., 2015; Thamdrup et al., 2019). These relationships define a spatially diffuse yet biogeochemically distinct CH_4-influenced zone, termed 'methanosphere', that may extend beyond the immediate seep zone, influencing adjacent off-seep ecosystems (Levin et al., 2016b).

Seepage intensity, seafloor topography, current regimes, and local biogeochemistry (foremost O_2) may influence aerobic CH_4 oxidation and with that the vertical and lateral extent of the methanosphere. As their metabolic electron acceptor, O_2 directly governs the activity and niche space of aerobic methanotrophs (Boetius & Wenzhöfer, 2013). Aerobic CH_4 oxidation may decline under severe O_2 depletion, where anaerobic CH_4 oxidation becomes increasingly important (Knittel & Boetius, 2009; Thamdrup et al., 2019). However, many aerobic methanotrophs remain highly active under microoxic conditions and can exhibit elevated oxidation rates at low O_2 concentrations because of their high affinity for O_2 (Steinle et al., 2017; Tavormina et al., 2013; Reis et al., 2024).

In the Southern California Borderland, multiple active CH_4 seep sites occur along faulted basins and ridges on the continental margin (~450-1050 m) (Hein et al., 2006; Maloney et al., 2015), where CH_4-rich fluids migrate upward and sustain communities of bacterial and folliculinid mats, clams, tubeworms, ampharetid polychaetes and carbonate rock-associated fauna (Grupe et al., 2015; Le et al., 2022; L. Levin et al., 2016). The waters surrrounding the Santa Monica, Del Mar, and Redondo Knoll seeps, for example, are characterized by varying O_2 concentrations with low values (<23µM) at seeps within the oxygen minimum zone as a result of high organic matter input and respiration in the water column (Grupe et al., 2015). These seeps serve as a natural laboratory to study the size of the pelagic methanosphere and the control of its scale by physical processes and biogeochemical parameters such as CH_4 bubble transport, CH_4 plume dynamics, lateral advection, and O_2 (Jordan et al., 2019; Ussler III et al., 2013). Understanding these control mechanisms is essential for defining the ecological footprint of cold seeps and quantifying their role in deep-sea carbon cycling.

https://doi.org/10.5194/egusphere-2026-4409
Preprint. Discussion started: 30 July 2026
© Author(s) 2026. CC BY 4.0 License.

To address this knowledge gaps, we tested the following hypotheses at three distinct active CH_4 seeps along the Southern California Borderland margin:

1. CH_4 concentrations and methanotroph indicators (*pmoA* gene abundance, community composition) remain elevated relative to background levels beyond the visible seep boundary.
2. Lower O_2 concentration enhances CH_4 oxidation and supports greater methanotroph abundance in the water column.
3. Physical transport processes, such as bottom current and bubble-mediated dispersal, contribute to the distribution of CH_4 and CH_4-oxidizing microbes into horizontally and vertically adjacent off-seep waters.

We used vertical, horizontal, and point source water column sampling with Niskin bottles via a CTD-rosette system and the human-occupied vehicle *Alvin* to study the distribution of CH_4 concentration, microbial CH_4 oxidation, microbial diversity, and pmoA gene abundance at on- and off-seeps locations. Our results suggest that CH_4 and methanotroph signatures extend beyond visible seep zones, with oxidation occurring across a range of O_2 conditions.

2 Methods

2.1 Study Areas

This study was conducted during a June–July 2023 expedition aboard the R/V *Atlantis* (AT50-12) where we investigated the spatial extent and structure of the pelagic methanosphere. We focused on three active CH_4 seeps along the Southern California Borderland margin (Fig. 1), Del Mar (~1020 m), Santa Monica 800-m Mound (~800 m), and Lasuen Knoll (~400 m), selected to represent a range of water depths, bottom-water O_2 concentrations, and regional current regimes at the time of sampling.

2.1.1 Del Mar Seep

The Del Mar Seep (Fig. 1a), ~30 km off Del Mar, California at 1020–1040 m depth, is positioned within strike-slip faults at the lower edge of the oxygen minimum zone (OMZ) boundary (Maloney et al., 2015; Ryan et al., 2012) and is overlaid with low-O_2 water (~17

https://doi.org/10.5194/egusphere-2026-4409
Preprint. Discussion started: 30 July 2026
© Author(s) 2026. CC BY 4.0 License.

µM O_2; (Grupe et al., 2015)). Seep-influenced sediment is characterized by sharp gradients in O_2, H_2S, and organic carbon (Maloney et al., 2015). Seepage activity varies, with a relatively inactive eastern edge, indicated by disarticulated, sparse clam beds and lack of bacterial mat or active gas venting (Maloney et al., 2015). In the western region, carbonate outcrops and chemosynthetic fauna dominate, and active CH_4-oxidizing archaea and bacteria are present (Mayr et al., 2025) (Maloney et al., 2015). Specifically, previous expeditions to the seep have identified authigenic carbonate boulders, dense bacterial mats and clam beds, tubeworm clusters, and *Bathysiphon filiformis* tube fields (Grupe et al., 2015; Le et al., 2022). Additionally, lower mean faunal $\delta^{13}C$ values were observed in sediment samples collected closer to the seep (<200 m), indicating that chemosynthetically derived carbon may support elevated animal biomass beyond the central seep zone (Grupe et al., 2015). Transplantation of carbonate rocks and associated fauna from active seepage to nearby off seep areas did not yield a change in macrofaunal density or diversity metrics after 25 months, although species composition was altered (Lee et al., 2025).

2.1.2 Santa Monica 800-m Mound

The Santa Monica 800-m Mound (Fig. 1b), referred to hereafter as Santa Monica Mound, lies in the Santa Monica Basin at ~800 m water depth, an area characterized by strong CH_4-rich seepage, the presence of gas hydrates, and blister-like seafloor deformation (Hein et al., 2006; Maloney et al., 2015; Paull et al., 2008). Periodic sampling and *in situ* surveys have documented persistent CH_4 bubbling and vigorous fluid flow across the 800-m mound (Paull et al., 1984). Located within the Santa Monica Basin OMZ, the semi-enclosed hydrography can restrict bottom-water exchange, leading to O_2 depletion (<3 µM O_2; (Kemnitz et al., 2020)) that enhances water column CH_4 oxidation and restricts benthic communities (Heintz et al., 2012; Lee, 2025). Specifically, water column methanotrophic activity was found to increases with restricted water circulation, peaking near the 737 m sill depth, where O_2-depleted waters support a psychrotolerant methanotrophic community (Heintz et al., 2012). At a nearby seep in the Santa Monica Basin, aragonite shells of potential chemosymbiotic bivalves exhibited pronounced ^{13}C depletion (−12‰ to −19‰ $\delta^{13}C$), consistent with incorporation of CH_4-derived carbon. Authigenic carbonate recovered from sediment cores was even more ^{13}C-depleted (−46‰ to −58‰ $\delta^{13}C$), indicating that carbon from AOM was the primary source (Hein et al., 2006).

https://doi.org/10.5194/egusphere-2026-4409
Preprint. Discussion started: 30 July 2026
© Author(s) 2026. CC BY 4.0 License.

2.1.3 Lasuen Knoll

Lasuen Knoll (Fig. 1b) is positioned within the Palos Verdes Fault Zone, a tectonically complex region that facilitates vertical fluid migration and supports the development of CH_4-rich habitats (Fisher et al., 2004; Thompson & Francis, 2019). Seismic mapping suggests that Lasuen Knoll is a pop-up structure at ~670 m depth at its base linked to a restraining stepover of the Palos Verdes Fault, with dextral shear transferring southeast through faults like Carlsbad Ridge and Coronado Bank (Thompson & Francis, 2019). As a relatively uncharacterized CH_4 cold seep, it is not known how CH_4 flux and activity vary spatially, or how it is influenced by faulting and localized overpressure zones. An exploratory dive by the Schmidt Ocean Institute was conducted in 2018 with the ROV SuBastian which visually identified carbonate outcrops, CH_4 bubbles, and potential CH_4 seep-associated fauna. Lasuen was revisited in July during FK210726 where the current seep site was discovered and some faunal sampling occurred (Lee et al., 2025; Pereira et al., 2026).

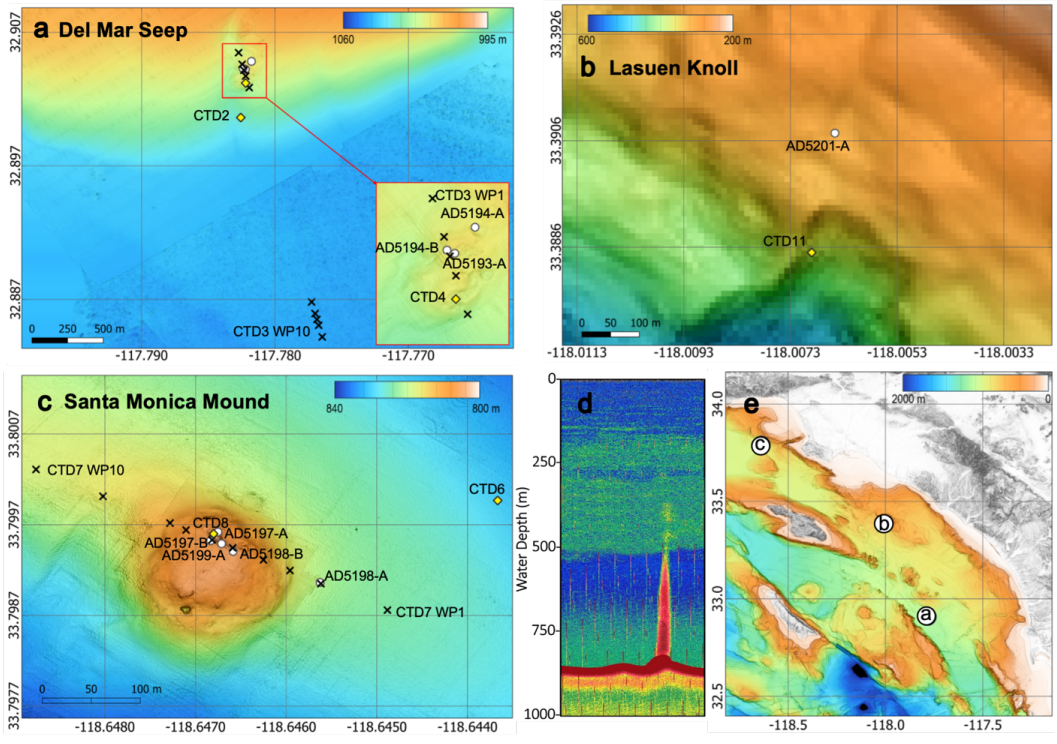

https://doi.org/10.5194/egusphere-2026-4409
Preprint. Discussion started: 30 July 2026
© Author(s) 2026. CC BY 4.0 License.

Figure 1. Bathymetric maps of (**a**) Del Mar Seep (northwest and ~1km away southeast seep regions), (**b**) Lasuen Knoll, and (**c**) the Santa Monica 800 m Mound, with (**d**) Santa Monica Mound EK80 backscatter profile of a CH_4 bubble plume observed at CTD8 and WP6 (CTD7) during cruise AT50-12. (**e**) showing site locations within the Southern California Borderland. Sampling stations from R/V Atlantis include vertical CTD casts (yellow diamonds) and horizontal CTD cast waypoints (black 'X'). Labeled waypoints include WP1 and WP10, with WP2–WP9 ordered sequentially between. HOV *Alvin* dive locations are indicated by white circles.

2.2 Bathymetric mapping

The three sites have varying scales of topographic and bottom character context provided by seafloor mapping (Figure 1). All have been surveyed using ship-mounted multibeam sonar, which resolves features in bathymetry and acoustic backscatter at scales of about 2% of water depth, or ~8 m for Lausen Knoll, ~16 m for Santa Monica Mound, and ~20 m for Del Mar Seep. The two deeper sites have also been surveyed using autonomous underwater vehicles (AUVs) (Caress et al., 2008) that map the seafloor with multibeam, sidescan, and subbottom profiler sonars from a 50 m altitude, providing 1-m-scale bathymetry and backscatter (Paull et al., 2008) that clearly delineate seep related features. The Del Mar Seep was surveyed by AUV in 2010, and the Santa Monica Mound in 2006, 2010, and 2018. The Santa Monica Mound was also surveyed from ROV *Ventana* in 2018 using an ROV-mounted Low Altitude Survey System (LASS) (Caress et al. 2025), which combines a subsea lidar laser scanner, multibeam sonar, and stereo color cameras flown at a 3 m altitude to produce 1-cm-scale topography and 0.2-cm-scale color photomosaics. In addition to revealing fine scale topographic features, the combined topography and photomosaic data maps the chemosynthetic community present at the Santa Monica Mound.

2.3 Sample collection

Sampling was conducted over two weeks during the AT50-12 expedition (July 16–29, 2023) aboard the R/V *Atlantis* using the HOV *Alvin* and a CTD/Rosette system for water column profiling and collection. Water samples were collected from various depths, spanning the surface to near-seafloor, across the three CH_4 seep sites using a rosette equipped with 23 × 10 L Niskin

https://doi.org/10.5194/egusphere-2026-4409
Preprint. Discussion started: 30 July 2026
© Author(s) 2026. CC BY 4.0 License.

bottles (Ocean Test Equipment, Inc., Fort Lauderdale, Florida). A Seabird Scientific pumped CTD system was mounted on a rosette frame outfitted with Niskin bottles and sensors to continuously measure conductivity (SBE4), temperature (SBE3), pressure (SBE9), dissolved O_2 (SBE43), fluorescence (FLNTURTD), and light transmission (C-Star). Salinity and density were calculated from conductivity and temperature, respectively, and depth was inferred from pressure. All sensors were calibrated prior to deployment according to manufacturer instructions.

Vertical CTD casts were deployed over active seep sites selected based on available information, which varied by location and included real-time EK80 acoustic backscatter data, multibeam seafloor mapping, and/or prior observations from *Alvin* dives. Horizontal CTD casts (TowYo's) collected water samples 5 m above the seafloor along a transect that contained on- and off-seep positions; off seep defined as no visible seep-associated fauna, microorganisms, or geophysical features. During movement along the transect, the CTD was kept 10 m above the seafloor and lowered to 5 m shortly only before closing, to flush the bottle with ambient water. For all casts, the ship maintained dynamic positioning using acoustic beacons to either remain on station despite prevailing currents (vertical CTD) or to move the CTD along the transect (horizontal CTD). At the Del Mar site, a noticeable gap in horizontal sampling reflects the transit between two spatially distinct, acoustically active seep features (the northwest and southeast region identified through bathymetry, Fig. 1a).

Samples collected by *Alvin* were obtained via Niskin bottles mounted on the submersible's basket. Sample locations were chosen based on either previously known coordinates (e.g., colonization arrays deployed at the Del Mar Seep during the WF05-21 expedition with the R/V *Western Flyer* and ROV *Doc Ricketts* (May 2021) and during FK210726 with remote operated vehicle (ROV) *Subastian* during Aug. 2021)) or observations of gas bubble releases (EK80 or *Alvin* observation) and chemosynthetic habitats during the dive. To prevent sediment contamination, Niskin bottles were triggered while the vehicle hovered approximately 0.5 m above the seafloor, just prior to contact and or after the observed current removed resuspended sediment. For all sampling events, water from each Niskin bottle was subsampled in the following order: (1) CH_4 concentration, (2) CH_4 oxidation rate, and (3) DNA preservation. A complete list of CTD casts and *Alvin* sample metadata is provided in Table 1 with the horizontal CTD cast waypoint metadata outlined in Table S1. All depths are reported as

https://doi.org/10.5194/egusphere-2026-4409
Preprint. Discussion started: 30 July 2026
© Author(s) 2026. CC BY 4.0 License.

meters below sea level, with "surface waters" defined as 1–5 m depth and "bottom waters" as 5–10 m above the seafloor.

Table 1. Summary of sampling events with Niskin bottles, including seep location, specific site characteristics (such as dominant seep organisms or gas releases), Alvin Dive/CTD no., sampling date, sampling start time (Alvin: Niskin closure, CTD: start of cast/transect), and geographic coordinates (latitude and longitude). Asterisks (*) indicate that multiple coordinates and corresponding depths were recorded across horizontal CTD transects, which can be found in Table S1. The sulfur mats are bacterial. Only the first waypoints for CTD3 and CTD7 are reported in Table 1. **(**DMS, Del Mar Seep; SMM, Santa Monica 800-m Mound; LK, Lasuen Knoll).

Site	Dive/CTD No.	Total Water Depth (m)	Latitude (dec. deg.)	Longitude (dec. deg.)	Sampling Date (UTC)	Sampling Start Time (UTC)	Site Characteristic
DMS	AD5193-A	1022	32.9042	-117.7822	2023-07-17	16:50	crabs, carbonate
	CTD 2	1044	32.8339	-117.7826	2023-07-17	22:45	frenulate worms
	AD5194-A	1022	32.9048	-117.7818	2023-07-18	17:30	brittle stars, snails
	AD5194-B	1019	32.9043	-117.7824	2023-07-18	20:30	carbonate, orange sulfur mat
	CTD 3*	1015	32.9055	-117.7827	2023-07-19	1:00	on-seep
	CTD 4	1036	32.9032	-117.7822	2023-07-19	23:50	across seep transect
SMM	AD5197-A	802	33.7996	-118.6468	2023-07-21	17:00	CH_4 bubbles, orange and white sulfur mat, carbonate
	AD5197-B	800	33.7995	-118.6468	2023-07-21	20:00	symbiotic clams
	CTD 6	827	33.7999	-118.6437	2023-07-22	3:30	off-seep
	AD5198-A	816	33.7991	-118.6456	2023-07-22	16:00	symbiotic clams, white sulfur mat
	AD5198-B	801	33.7994	-118.6466	2023-07-22	19:30	carbonate ledge, ampharetid worm bed
	CTD 7*	816	33.7988	-118.6449	2023-07-23	3:40	across seep transect
	AD5199-A	800	33.7995	-118.6467	2023-07-23	16:30	CH_4 plume, carbonate, orange sulfur mat
	CTD 8	800	33.7996	-118.6468	2023-07-24	2:20	CH_4 plume
LK	CTD 11	387	33.3885	-118.0069	2023-07-26	3:30	on-seep
	AD5201-A	310	33.3907	-118.0065	2023-07-26	15:45	no obvious seep features

2.4 CH_4 Concentration

Water column CH_4 samples were collected in 100 mL glass vials sealed with grey butyl stoppers and aluminum crimp caps, filling each vial three times to eliminate air bubbles before final sealing. Vials for CH_4 determination were injected with 7.5 mL of 50% NaOH and a 2.5 mL air headspace while a total volume of 10 ml water sample was removed. The partial pressure

https://doi.org/10.5194/egusphere-2026-4409
Preprint. Discussion started: 30 July 2026
© Author(s) 2026. CC BY 4.0 License.

of CH_4 in the headspace was subsequently analyzed via gas chromatography. Specifically, a Shimadzu Gas Chromatograph (GC-2014) was used, equipped with a Haysep-D packed column and a flame ionization detector. The column temperature was set to 80 °C, and helium served as the carrier gas at a flow rate of 12 mL per minute. CH_4 concentrations were calibrated using CH_4 standards (Scotty Analyzed Gases), with a precision of ±5%. Sulfate samples were analyzed via ion chromatography (Metrohm 761). Water column CH_4 concentrations were calculated using Henry's law and the Bunsen solubility coefficient (Yamamoto et al., 1976) to account for CH_4 in both the gas and liquid phase of the preserved samples.

2.5 Radiotracer incubations for the determinations of microbial CH_4 oxidation

Water column CH_4 oxidation samples were collected in 30 mL glass vials sealed with non-toxic chlorobutyl stoppers (blue Bellco stoppers, 20 mm, (Niemann et al., 2015)) filling each vial three times to eliminate air bubbles before final sealing. CH_4 oxidation rates were determined onboard through *ex situ* incubations with tritium-labelled CH_4 (^3H-CH_4) applying established methods (Bussmann et al., 2015). Samples (triplicates) were incubated between 35 and 88 hours (depending on sample set) with 10 µL gaseous ^3H-CH_4 (~2 kBq, specific activity 20 Ci/mmol, American Radiolabeled Chemicals, USA). Control samples were injected with 100 µL of 25% H_2SO_4 prior to radiotracer injection to stop microbial activity. To determine the total radioactivity of the sample, the crimped vials were opened, and a 2 mL subsample was pipetted into a 6 mL scintillation vial and filled with 3 mL of Ultima Gold LLT scintillation cocktail from Perkin Elmer. For the determination of ^3H-CH_4 that was metabolized to ^3H-H_2O, 2 mL from the incubation was subsampled into an additional 6 mL scintillation vial and bubbled with air for 5 minutes to remove ^3H-CH_4 prior to the addition of the scintillation cocktail. Both subsamples were mixed by gentle inversion and counted onboard in a Perkin Elmer Tri-Carb liquid scintillation counter. The *in situ* temperatures of the samples ranged from ~4 to 20°C. Due to the availability of only a single incubator, all samples were incubated at 6 °C. in the dark. To correct for abiotic tracer turnover, rates were considered detectable only when they exceeded the mean tracer turnover measured in killed controls by more than one standard deviation. For samples meeting this criterion, the mean killed-control value was subtracted from the measured rate. Assuming first-order kinetics, the rate constant (k) was determined using the following equation:

https://doi.org/10.5194/egusphere-2026-4409
Preprint. Discussion started: 30 July 2026
© Author(s) 2026. CC BY 4.0 License.

$$k = \frac{^3H - H_2O}{[(^3H - H_2O \ + \ ^3H - CH_4) \ \cdot \ t]}$$

In this equation, ^3H-H_2O refers to the amount of tritiated water produced (in counts per minute, cpm), ^3H-CH_4 represents the remaining unoxidized tritiated CH_4 (cpm), and t is the incubation duration in days. CH_4 turnover time was calculated as the inverse of the fractional turnover rate ($1/k$), equivalent to the CH_4 concentration divided by the oxidation rate (r_{ox}) ($[CH_4]/r_{ox}$), under the assumption of prolonged water mass residence with limited mixing (Heintz et al., 2012).

CH_4 oxidation rates (r_{ox}) were calculated again assuming first-order kinetics, using the fractional turnover rate multiplied by the CH_4 concentration (nM). Rates were determined with the following equation:

$$r_{ox} = k \cdot \ [CH_4]$$

2.6 DNA Extraction

Seawater was collected into pre-rinsed 1.5 L polycarbonate bottles and stored shortly at 6 °C until filtration. Microbial biomass was collected by filtering the samples using a peristaltic pump through 0.22 µm Sterivex filters (Millipore, Cat. No. SVGP0150). Filters were immediately frozen after filtration for downstream molecular analyses. Genomic DNA was extracted from Sterivex filters using a modified phenol–chloroform procedure followed by purification on Zymo silica spin columns (part C1006). Briefly, each filter was sealed, and 1.8 mL of filter-sterilized lysis buffer (containing 50 mM EDTA, 50 mM Tris–Cl [pH 8], 0.75 M sucrose, and 0.01% Tween 20) was injected into the cartridge. Lysozyme (40 µL; 50 mg mL^{-1}) was then added, and the filter was incubated at 37 °C for 45 min under rotation. 50µL of Proteinase K (800 U mL^{-1}) and 150 µL of 20% SDS were added to achieve a final SDS concentration of ~1%, followed by incubation at 55°C for 2 hr. The lysate was transferred to a polypropylene tube, and total nucleic acids were extracted via successive phenol–chloroform–isoamyl alcohol (25:24:1) extractions at 65°C, with centrifugation steps (10 min at 16,000 × g) to separate the aqueous and organic phases. Residual phenol was removed through an additional chloroform–isoamyl alcohol wash, and DNA was precipitated with 0.4 vol of 5 M NaCl and 0.8 vol of isopropanol. The precipitated DNA was bound to Zymo Spin-Away columns by

https://doi.org/10.5194/egusphere-2026-4409
Preprint. Discussion started: 30 July 2026
© Author(s) 2026. CC BY 4.0 License.

repeated loading at 6,000 × g for 1 min, washed with 70% ethanol, and eluted in nuclease-free water or 10 mM Tris. Final DNA extracts were stored at −80 °C until further analysis.

2.7 PCR and Illumina MiSeq sequencing of the 16s rRNA gene

The V4-V5 region of the 16S rRNA gene was amplified using 515F and 926R (Parada et al., 2016) archaeal/bacterial primers with Illumina adapters (515F 5'-TCGTCGGCAGCGTCAGATGTGTATAAGAGACAG-GTGYCAGCMGCCGCGGTAA-3'; 926R 5'-GTCTCGTGGGCTCGGAGATGTGTATAAGAGACAG-CCGYCAATTYMTTTRAGTTT-3'). PCR reactions were completed with Q5 Hot Start High-Fidelity 2x Master Mix (New England Biolabs, USA) in 15 µL reaction volumes according to manufacturer's directions with the following cycle parameters: 2 min at 98C followed by 31 cycles of 98°C for 10s, 54°C for 20s, 72°C for 20s, with an extra final elongation step of 72°C for 2 min. PCR samples were pooled and barcoded with Illumina Nextera XT index 2 primers that include unique 8-bp barcodes (P5 5'-AATGATACGGCGACCACCGAGATCTACAC-XXXXXXXX-TCGTCGGCAGCGTC-3'; P7 5'-CAAGCAGAAGACGGCATACGAGAT-XXXXXXXX-GTCTCGTGGGCTCGG-3') using Q5 Hot Start with 3 µL pooled PCR product added to a 30 µL reaction volume, annealed at 66°C, and cycled 11 times. Products were run on 1.5% agarose gel and quantified by band intensity. Barcoded PCR products were combined in equimolar amounts and 300uL of this combined sample was run on 1.5% low melt agarose gel and purified with Promega's Wizard SV Gel and PCR Clean-up System, Promega#A9281. Sample was sequenced by Laragen (Culver City, CA, USA) using MiSeq Reagent Kit v3 (600-cycle) #MS-102-3003 on Illumina's MiSeq platform with the addition of 15-20% PhiX.

2.8 Sequence processing and taxonomic analysis

The Illumina-sequenced paired-end fastq files were processed using DADA2 for amplicon sequence variant (ASV) calling (Callahan et al., 2016) based on developer recommendations and Cutadapt v3.4 for sequence quality trimming and primer removal (Martin, 2011). Reads that did not assemble in the overlapping region or that failed to meet the q-score threshold of 30 were removed from subsequent analyses. Taxonomy was assigned to 16S rRNA sequences via alignment to SILVA Train Set v138.2 amended with plastid sequences annotated with host taxonomy (Eitel et al., 2024). Raw reads are available on NCBI SRA under BioProject

https://doi.org/10.5194/egusphere-2026-4409
Preprint. Discussion started: 30 July 2026
© Author(s) 2026. CC BY 4.0 License.

PRJNA1479037 at accessions SRR39191919-SRR39191890. See Supporting Information for additional information on read retention and all parameters used during DADA2.

2.9 Quantitative PCR

For the qPCR assays, each 10 µL reaction consisted of 5 µL Phusion SYBR® Green PCR Master Mix (BioRad), 0.5 µL (0.5 µM) each primer, 3.5 µL PCR-grade H_2O and 0.5 µL of DNA (concentration pre-determined through Qubit™ dsDNA Quantification, High Sensitivity Assay Kit). Duplicate bacterial pmoA assays were run using water column specific primers wcpmoA189f and wcpmoA661r (Tavormina et al., 2008) and the following cycling parameters: 98°C for 2 min followed by 40 cycles of 98°C for 10s, 52°C for 20s, 72°C for 30s, detection, then a melt curve from 65°C to 95°C in 0.5C increments, plate reading every 5s. Standard curves were constructed with 10-fold dilutions of PCR products from 0 (negative control) to 10^6 gene copies total DNA from extracted *Methylomonas* sp. LW13 cells.

2.10 Spearman rank correlation

Spearman rank correlation analyses were conducted to evaluate monotonic relationships among environmental and biogeochemical variables, including depth, CH_4 oxidation rate constant (k), CH_4 turnover time, dissolved CH_4 concentration, dissolved O_2 concentration, temperature, pmoA gene abundance (log copies L^{-1}), and fluorescence (µg L^{-1}). Analyses were performed separately for each seep site (Del Mar Seep, Santa Monica Mound, and Lasuen Knoll). To ensure consistency across variables, only samples with complete data for all parameters were included (listwise deletion). Spearman's rank correlation coefficients (ρ) were calculated using non-parametric methods that do not assume normality. Correlation matrices were visualized as heatmaps, with coefficients ranging from −1 to +1.

3 Results

Hydrographic and biogeochemical parameters in the water column

Hydrographic profiles revealed pronounced vertical gradients in temperature, salinity, and density across all sites, shaped by strong upper-ocean stratification and well-defined pycnoclines (Fig. 2a–d). At Del Mar Seep (CTD4, 1035 m), a sharp pycnocline occurred between ~50–150 m, where temperature dropped rapidly from ~18 to 8 °C, salinity increased from ~33.1

https://doi.org/10.5194/egusphere-2026-4409
Preprint. Discussion started: 30 July 2026
© Author(s) 2026. CC BY 4.0 License.

to ~34.1 PSU, and density rose from ~1023 to ~1027.5 kg m^{-3}. Below this zone, gradients were more gradual, reaching 3.9 °C, 34.48 PSU, and 1032.2 kg m^{-3} near the seafloor. Similar stratification was observed at Santa Monica off-seep (CTD6, 820 m) and Santa Monica Mound (CTD8, 799 m), with strong thermoclines and haloclines in the upper ~100–150 m, followed by more linear deep-water gradients. Near-bottom values converged around 5.3 °C, 34.38 PSU, and ~1030.8–1030.9 kg m^{-3}. The shallower Lasuen Knoll site (CTD11, 382 m) showed a compressed but still distinct pycnocline from ~25–100 m, with temperature declining from ~19.6 to ~10 °C, salinity increasing from ~33.2 to 34.2 PSU, and density rising from ~1023.7 to 1028.4 kg m^{-3}.

Optical profiles revealed vertical structure in fluorescence and beam transmission at all sites (Fig. 2e–h). At Del Mar Seep (CTD4, 1035 m), a sharp subsurface fluorescence peak (1.29 µg L^{-1}) was observed at 33 m, with values declining steeply through the upper ~100 m and tapering more gradually to 0.034 µg L^{-1} near the seafloor. Beam transmission was at 95.8% at the surface, decreased to 92.4% at 34 m below sea level, then increased to ~97% by 800 m with a slight decline in the bottom 100 m, marking the presence of a benthic nepheloid layer. Similar fluorescence profiles were observed at Santa Monica off-seep (CTD6, 820 m), where a 1.29 µg L^{-1} peak occurred at 41 m, decreasing steadily to 0.041 µg L^{-1} at depth. Transmission increased to ~96.5% but also dipped slightly near the bottom. At Santa Monica Mound (CTD8, 799 m), fluorescence peaked at 0.81 µg L^{-1} at 34 m, with a similar decline to 0.040 µg L^{-1} at depth. Transmission followed the same pattern, increasing from 92.3% to ~96.2% with a small downturn near the seafloor. Lasuen Knoll (CTD11, 382 m) exhibited the highest surface fluorescence (1.82 µg L^{-1} at 34 m), declining steadily to 0.021 µg L^{-1} at depth, with beam transmission increasing from 92.0% to 96.8% before also decreasing slightly near bottom.

Dissolved CH_4 and O_2 profiles varied in magnitude across seep sites but generally showed similar vertical structure (Fig. 2i–l). Near-surface CH_4 concentrations exceeded atmospheric equilibrium at all sites, with values ranging from 33 to 99 nM in the upper 3 m. At Del Mar Seep (CTD4), CH_4 peaked at 131 nM at 1026 m and was 47 nM at 3 m. O_2 decreased from 231.5 µM at the surface to a minimum of 9.2 µM at 715 m, then increased slightly to 22.7 µM at 1035 m. Santa Monica off-seep (CTD6) exhibited the highest CH_4 concentration in the CTD dataset across all sites, reaching 797 nM at 804 m; this deep value was confirmed by three replicate headspace measurements. Surface CH_4 was 99 nM at 2 m. O_2 declined from 232.8 µM at the surface to 3.9 µM at 820 m. At Santa Monica Mound (CTD8), CH_4 peaked at

https://doi.org/10.5194/egusphere-2026-4409
Preprint. Discussion started: 30 July 2026
© Author(s) 2026. CC BY 4.0 License.

293 nM at 798 m, with 82 nM at 3 m. O_2 ranged from 253.4 µM at the surface to 3.5 µM at 799 m; this cast intersected the EK80 CH_4 plume. At Lasuen Knoll (CTD11), CH_4 increased from 33 nM at 3 m to a maximum of 214 nM at 360 m, then declined to 127 nM at 382 m. O_2 concentrations decreased from 236.7 µM at the surface to 32.1 µM at 378 m. The relatively higher near-bottom O_2 at Lasuen reflects the shallower sampling depth and less intense depletion compared to deeper sites.

CH_4 oxidation rates varied across sites and depths and were generally elevated near CH_4 concentration maxima and within O_2-limited strata (Fig. 2m–p). At Del Mar Seep (CTD4), oxidation peaked at 0.34 nmol L^{-1} d^{-1} at 1005 m, with measurable activity at the surface (up to 0.15 nmol L^{-1} d^{-1} at 2 m). These depths corresponded to CH_4 concentrations between 75–131 nM and O_2 levels ranging from 22.7 µM near the bottom to a minimum of 9.2 µM at 715 m. At Santa Monica off-seep (CTD6), oxidation reached 1.50 nmol L^{-1} d^{-1} at 804 m, where CH_4 was 797 nM and O_2 was 3.9 µM. Average oxidation across 804–819 m ranged from 0.50 to 1.18 nmol L^{-1} d^{-1}. At Santa Monica Mound (CTD8), oxidation rates were highest overall, reaching 4.98 nmol L^{-1} d^{-1} at 791 m where CH_4 was 235 nM and O_2 was 3.5 µM. Lasuen Knoll (CTD11) showed lower oxidation activity, peaking at 0.76 nmol L^{-1} d^{-1} at 201 m at CH_4 concentrations of 62 nM and a minimum O_2 of 32.1 µM. In all cases, peak CH_4 oxidation occurred 13 to 30 m above the seafloor, rather than at the deepest sampling depth, which was ~5 m above bottom. These maxima generally aligned with elevated CH_4 concentrations and reduced O_2 levels. At Lasuen Knoll, the oxidation maximum was located much higher in the water column, at 201 m (~186 m above the seafloor).

https://doi.org/10.5194/egusphere-2026-4409
Preprint. Discussion started: 30 July 2026
© Author(s) 2026. CC BY 4.0 License.

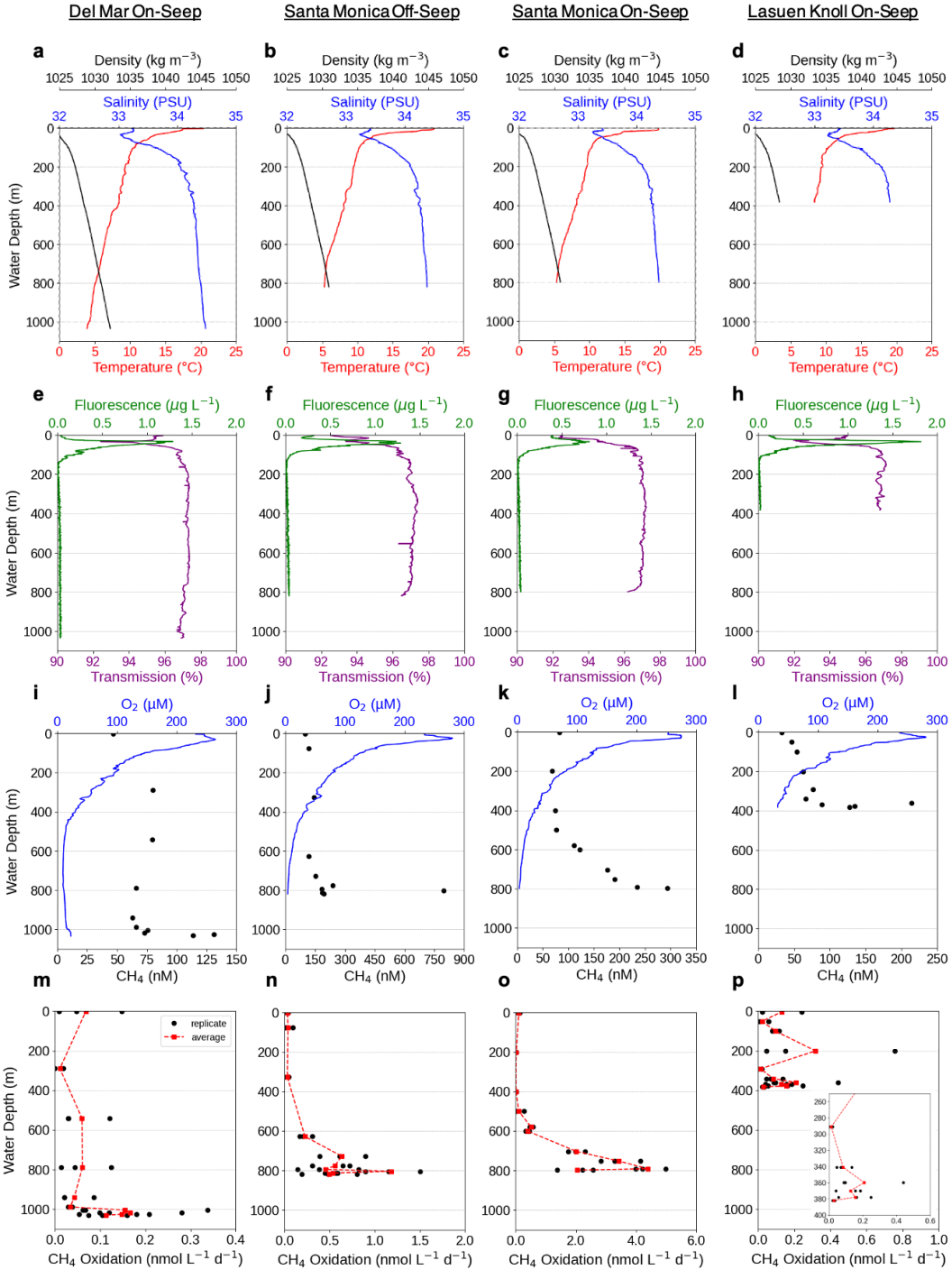

https://doi.org/10.5194/egusphere-2026-4409
Preprint. Discussion started: 30 July 2026
© Author(s) 2026. CC BY 4.0 License.

Figure 2. Vertical profiles of hydrographic and biogeochemical parameters in the water column at the Del Mar seep (left panels; seafloor at 1036 m), Santa Monica off-seep (center-left panels; seafloor at 827 m), Santa Monica Mound on-seep (center-right panels; seafloor at 800 m), and Lasuen Knoll (right panels; seafloor at 387 m) seep sites. Panels (**a–d**) show density (black, top x-axis), salinity (blue, top x-axis), and temperature (red, bottom x-axis). Panels (**e–h**) show chlorophyll-a fluorescence (green, bottom x-axis), reported in µg L^{-1} as a proxy for phytoplankton biomass, and beam transmission (magenta, top x-axis). Panels (**i–l**) show dissolved CH_4 concentrations (black circles, left x-axis) and dissolved O_2 (blue, right x-axis). Panels (**m–p**) display CH_4 oxidation rates measured in triplicate (black circles), with average rates shown as red squares connected by dashed lines. Note the differences in x-axis scales among CH_4 and CH_4 oxidation variables, and depth in the inset of Fig. 2p. All data were collected from vertical CTD casts (casts 4, 6, 8, and 11, respectively) at the sites indicated in Table 1 and Fig. 1 on the Southern California margin.

CH_4 oxidation rates and dissolved CH_4 concentrations fluctuated across a horizontal transect sampled 5 m above the seafloor across Del Mar Seep (~2.4 km track; Fig. 3a). Oxidation was highest at WP1 (0 m along track; up to 2.56 nmol L^{-1} d^{-1}) at the northwestern end of the transect, where CH_4 was 92.4 nM and O_2 was 17.9 µM. Rates declined at WP2 and WP3 (0.29 and 0.36 nmol L^{-1} d^{-1} at 102 and 150 m; CH_4: 77.0 nM), with WP3 corresponding to the center of the northwestern seep site. Beyond 200 m across the track, oxidation remained lower (0.16–0.20 nmol L^{-1} d^{-1}; CH_4: 64.9–80.9 nM), with the lowest rates and concentrations observed between WP6 and WP10 (0.07–0.20 nmol L^{-1} d^{-1}; 42.7–66.6 nM). A modest increase in rates at WP8 (2284 m along track; 0.19 nmol L^{-1} d^{-1}; 55.0 nM) likely reflects a less active southeastern seep site, which was identified through high-resolution bathymetric mapping. O_2 concentrations across the transect ranged from ~16 to 22 µM. These patterns highlight the spatial heterogeneity of CH_4 oxidation across the seep field and indicate that peak water column microbial activity does not necessarily coincide with areas of strongest visible seep signs (e.g., carbonates, sulfur bacteria mats).

At Santa Monica Mound, CH_4 oxidation rates and concentrations varied across a ~400 m transect sampled 5 m above the seafloor (800–816 m water depth; CTD7; Fig. 3b). The CH_4 plume was centered at WP6 (193 m across the track), and a directional bottom current inferred

https://doi.org/10.5194/egusphere-2026-4409
Preprint. Discussion started: 30 July 2026
© Author(s) 2026. CC BY 4.0 License.

from plume curvature in sonar data. WP1 and WP2 (0 and 73 m across the track respectively) were located off-mound to the southeast, while WP9 and WP10 (317 and 399 m across the track respectively) were off-mound to the northwest. WP3 through WP8 (112–245 m across the track) spanned the mound crest and encompassed the visibly active seepage zone. CH_4 oxidation was moderate off-mound at WP1 and WP2 (1.46 and 1.33 nmol L^{-1} d^{-1}; CH_4: 141.6 and 147.4 nM) and increased across the mound crest (1.27–2.61 nmol L^{-1} d^{-1}; CH_4: 107.9–194.4 nM). WP3 marked a local CH_4 maximum (194.4 nM; 1.75 nmol L^{-1} d^{-1}), and WP6 intersected the sonar-detected CH_4 plume (192.4 nM; 2.29 nmol L^{-1} d^{-1}). The highest oxidation rate occurred at WP10 (3.54 nmol L^{-1} d^{-1}), followed by elevated activity at WP9. O_2 ranged from ~3.3 to 4.0 µM across the transect. Overall, oxidation increased from WP1 to WP10, with peak activity observed at off-mound sites 100 to 150 m beyond the visibly active seep zone similar to the Del Mar transect.

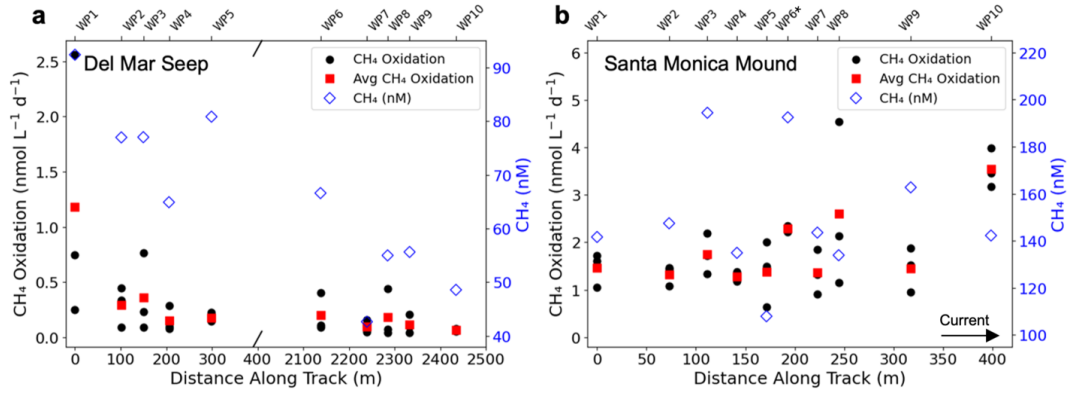

Figure 3. Both (**a**) and (**b**) represent a near seafloor (5 m above) lateral transect of CH_4 concentration and CH_4 oxidation rates across (**a**) Del Mar Seep (WP3) and a visibly less active separate seep location (WP8) (CTD3), and (**b**) Santa Monica Mound (WP1–10; CTD7). CH_4 oxidation (black circles) and average CH_4 oxidation (red squares) are shown on the left y-axes; dissolved CH_4 concentrations (blue diamonds) on the right y-axes. For the Del Mar Seep, off-seep sites are WP1 and WP5 as well as W6 and WP10. The Santa Monica Mound is located from WP3 to WP8. Panel (**a**) shows a broken x-axis to accommodate distant sampling locations. At Santa Monica Mound, the CH_4 plume (*) detected by EK80 echosounder data was centered near WP6, and the bottom current was inferred to flow from WP1 toward WP10. Note the distinct x-axis scales in each panel. See text for details.

https://doi.org/10.5194/egusphere-2026-4409
Preprint. Discussion started: 30 July 2026
© Author(s) 2026. CC BY 4.0 License.

Methanotrophic activity in the near-seafloor water column

Water column samples near the seafloor (0.5 m above bottom) were collected using the *Alvin* submersible. The ^{3}H-CH_4 *ex situ* incubations revealed a wide range of CH_4 oxidation rates, indicating substantial spatial heterogeneity across sites (Table 2). At Del Mar Seep, three stations (AD5193-A, AD5194-A, AD5194-B) within 200 m of the seep center showed moderate CH_4 oxidation (0.31–0.64 nmol L^{-1} d^{-1}) and concentrations (74–190 nM). AD5193-A was sampled above seep carbonates inhabited by lithodid crabs, while AD5194-A featured ophiuroids and buccinid gastropods. AD5194-B was positioned adjacent to a patch of orange sulfur bacterial mat. Although faunal composition and mat presence varied, CH_4 levels and oxidation rates remained within a similar range.

In contrast, Santa Monica Mound exhibited greater variability across five stations. AD5197-A, located near white and orange sulfur bacterial mats and carbonate outcrops with intermittent CH_4 bubbling, had elevated CH_4 (1.3×10^4 nM) and an intermediate oxidation rate (52 nmol L^{-1} d^{-1}). AD5197-B, sampled from a bed of symbiont-bearing clams lacking mat and carbonate cover, showed lower CH_4 (109 nM) and oxidation (0.32 nmol L^{-1} d^{-1}). AD5198-A (off-mound) and AD5198-B had moderate CH_4 concentrations (149–183 nM) and oxidation rates (0.20–0.77 nmol L^{-1} d^{-1}), corresponding to patchy mat and carbonate habitats. The highest values occurred at AD5199-A, sampled within an intense CH_4 bubble plume (EK80-detected; Fig. 1e), with a CH_4 concentration of 2.5×10^5 nM and an oxidation rate of 454 nmol L^{-1} d^{-1}. This station also had extensive sulfur bacterial mat cover and carbonate substrate.

At Lasuen Knoll, the single station AD5201-A lacked visible seep structures but showed signs of recent slope disturbance. CH_4 concentration was 133 nM, and oxidation was 0.84 nmol L^{-1} d^{-1}, values consistent with low-intensity seepage in the absence of visible seep structures. However, active seepage with seep biota were identified on subsequent dives at locations on Lasuen. Overall, CH_4 oxidation and concentrations varied both within and among seep fields, including measurable methanotrophic activity at sites over 100 meters from the seeps, lacking strong visual indicators of seepage such as sulfur bacterial mat or carbonates.

https://doi.org/10.5194/egusphere-2026-4409
Preprint. Discussion started: 30 July 2026
© Author(s) 2026. CC BY 4.0 License.

Table 2. Summary of *Alvin* sampling stations for Del Mar Seep (DMS), Santa Monica Mound (SMM), and Lasuen Knoll (LK) including the average CH_4 oxidation rates, corresponding CH_4 concentrations and environmental features.

Location	Niskin ID	CH_4 (nM)	Avg CH_4 Oxidation (nmol L^{-1} d^{-1})	Standard Deviation (± nmol L^{-1} d^{-1})	Site Characteristic
DMS	AD5193-A	190	0.31	0.38	crabs, carbonate
	AD5194-A	85	0.64	0.75	brittle stars, snails
	AD5194-B	74	0.64	0.17	carbonate, orange sulfur mat
SMM	AD5197-A	1.3×10^4	52	24	CH_4 bubbles, orange and white sulfur mat, carbonate
	AD5197-B	109	0.32	0.13	symbiotic clams
	AD5198-A	149	0.20	0.13	symbiotic clams, white sulfur mat
	AD5198-B	183	0.77	0.24	carbonate ledge, ampharetid worm bed
	AD5199-A	2.5×10^5	454	121	CH_4 plume, carbonate, orange sulfur mat
LK	AD5201-A	133	0.84	0.73	no obvious seep features

Rate constant and CH_4 turnover times

CH_4 oxidation rate constants (k) and corresponding turnover times were calculated from a subset of Niskin bottles collected during vertical CTD casts at Del Mar Seep (CTD4), Santa Monica Mound (CTD8), and Lasuen Knoll (CTD11), as well as paired *Alvin* Niskin samples. Results from selected depths are presented in Table 3. The full dataset for each vertical CTD cast is listed in Table S2. Turnover times varied by site and depth, ranging from as short as 0.32 years to as long as 19.3 years. At Del Mar Seep, turnover times ranged from 1.73 years near the surface (2 m depth) to 0.32 years above the seafloor at AD5194-A. A midwater sample at 290 m showed the longest turnover time (19.3 years), corresponding to a CH_4 minimum and elevated O_2. At Santa Monica Mound, turnover was relatively fast at the surface (2.18 years at 2 m) and above the seafloor (0.40–1.47 years), with slower turnover observed at 200 m (10.1 years). At Lasuen Knoll, turnover times ranged from 0.48 to 11.9 years, with the longest value at 382 m and shorter turnover times both near the surface and above the seafloor. Across all three sites, shorter CH_4 turnover times were typically observed near the seafloor and surface, while slower turnover occurred at intermediate depths.

https://doi.org/10.5194/egusphere-2026-4409
Preprint. Discussion started: 30 July 2026
© Author(s) 2026. CC BY 4.0 License.

Table 3. Depth-dependent measurements of O_2, CH_4, CH_4 oxidation rate constants (k), and resulting turnover times for Del Mar Seep (DMS), Santa Monica Mound (SMM), and Lasuen Knoll (LK). (*) denotes the O_2 concentration and temperature are estimated from the vertical CTD profile at the corresponding depth and site (CTD4 for DMS, CTD8 for SMM, and CTD11 for LK). The *Alvin* samples were taken 0.5 m above seafloor and the deepest CTD Niskin in each cast was collected 5 m above the seafloor.

Location	CTD/Niskin ID	Water depth (m)	O_2 (µM)	CH_4 (nM)	Temp (°C)	Rate constant (k)	Turnover Time (y)
DMS	4	2	237	21	20.4	1.6×10^{-3}	1.73
DMS	4	290	58	36	8.95	1.4×10^{-4}	19.3
DMS	4	1031	22	51	3.96	8.4×10^{-4}	3.15
DMS	AD5194-A	1022	20*	39	3.96*	8.3×10^{-3}	0.321
SMM	8	2	260	37	19.8	1.3×10^{-3}	2.18
SMM	8	200	103	31	3.69	2.7×10^{-4}	10.1
SMM	8	798	3.3	132	5.30	6.8×10^{-3}	0.404
SMM	AD5199-A	799	3.3*	9.8×10^{4}	5.30*	1.9×10^{-3}	1.47
LK	11	3	243	15	19.6	4.2×10^{-3}	0.719
LK	11	201	75	28	9.52	4.9×10^{-3}	0.563
LK	11	382	33.0	57.36	8.36	2.3×10^{-4}	11.9
LK	AD5201-A	310.432	46*	60	8.8*	5.7×10^{-3}	0.477

3.4 Microbial community composition in the water column

Analysis of amplicon 16S rRNA gene sequences from water column samples collected above the seep sites, spanning the euphotic zone to near-bottom waters, revealed that the dominant bacterial and archaeal taxa included Thermoplasmatota, Crenarchaeota, Proteobacteria, Cyanobacteria, and Planctomycetota. While Thermoplasmatota was the most prevalent overall, the relative distributions of these phyla varied by seep site and water column depth (e.g., ~18% at Del Mar Seep, ~43% at Santa Monica Mound, and ~36% at Lasuen Knoll for Thermoplasmatota average relative abundance). Notably, Proteobacteria, including Oceanospirillales_7, Alteromonadales, Thiomicrospirales, and Arenicellales, were particularly

https://doi.org/10.5194/egusphere-2026-4409
Preprint. Discussion started: 30 July 2026
© Author(s) 2026. CC BY 4.0 License.

well represented in mid- and deepwater samples, consistent with the broad metabolic versatility characteristic of this phylum. In surface waters, the phototrophic primary producers within the order Synechococcales were highly abundant, accounting for 77% of the microbial community at Del Mar Seep and 60% at Santa Monica Mound, suggesting a significant contribution of cyanobacterial primary production (Fig. 4). Flavobacteriales was the second most abundant order in the surface water at Del Mar Seep (3.7%) and Santa Monica Mound (4.8%). Members of this group are known for their role in the decomposition of organic matter and utilizing dissolved organic carbon from phytoplankton blooms (Pontiller et al., 2022). Archaeal orders including Marine Group II (Thermoplasmatota) and Nitrosopumilales (Crenarchaeota) were the dominant taxa in most samples. The prevalence of Nitrosopumilales, an order characterized by ammonia-oxidizing archaea, aligned with their near absence in surface waters above the OMZ. Among bacterial orders, Oceanospirillales_7 was abundant in mid- and deep-water samples at Del Mar Seep and detected at lower abundances at Santa Monica Mound and Lasuen Knoll. Nitrincolaceae, the predominant family found within Oceanospirillales_7, are heterotrophic bacteria that include many known alkane oxidizers and play a role in organic matter degradation, sulfur compound metabolism, and nitrogen cycling (Liu et al., 2019). Flavobacteriales, in addition to its presence in the surface water, was prevalent throughout the water column of Del Mar seep and near the seafloor of Santa Monica Mound (AD5198-A; 20.7% relative abundance) and Lasuen Knoll (AD5201). Thiomicrospirales, an order containing many sulfur-oxidizing bacteria, was abundant in deep samples across all three seep sites, including Lasuen Knoll, with the highest relative abundance in the bottom waters of Santa Monica Mound (11.3%). In contrast to other microbial groups associated with hypoxic and anoxic environments, such as ammonia- or nitrite-oxidizing taxa, Thiomicrospirales exhibited a more restricted vertical distribution, with peak abundances occurring in deeper water. Orders that contain methanotrophs (e.g., Burkholderiales) did not show a noticeable increase at active seepage sites. However, any such signal was likely obscured by the presence of non-methanotrophic members within the order.

https://doi.org/10.5194/egusphere-2026-4409
Preprint. Discussion started: 30 July 2026
© Author(s) 2026. CC BY 4.0 License.

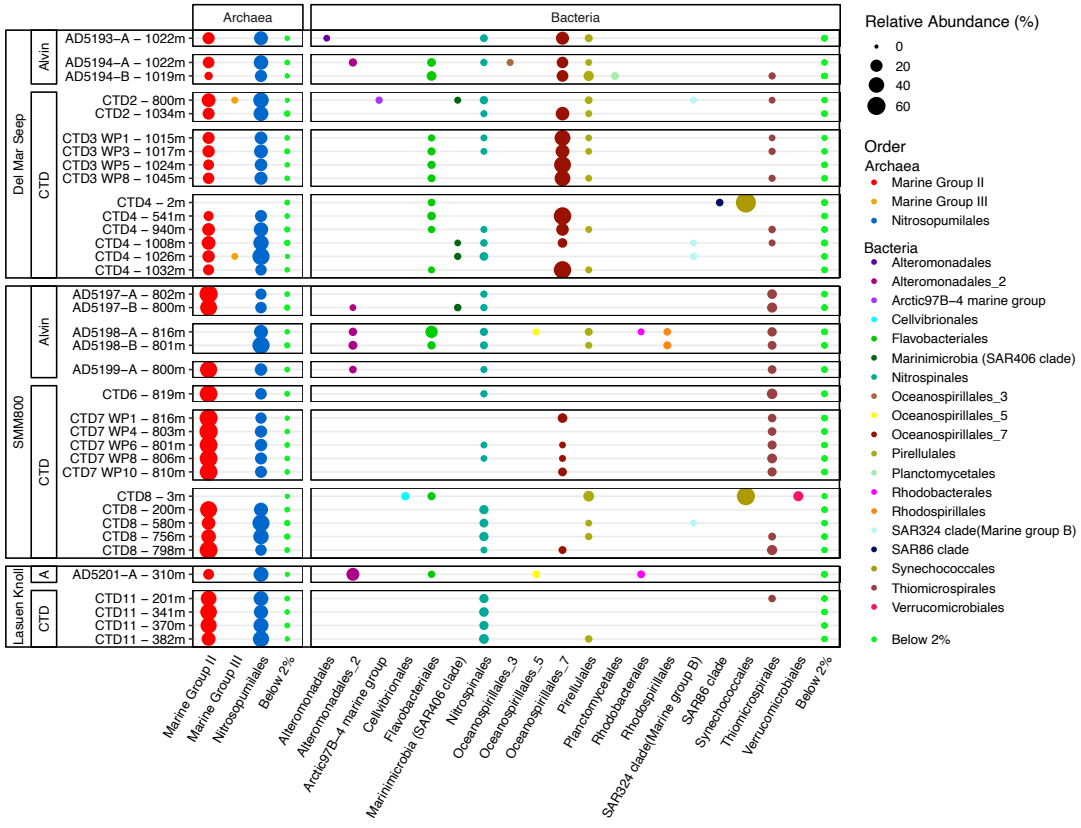

603

604 **Figure 4**. Microbial community composition from CTD and *Alvin* Niskin samples from Del Mar
605 Seep, Santa Monica Mound, and Lasuen Knoll. Dot size shows the relative abundance (%) of
606 microbial orders (columns, colors) in samples (rows). Samples are grouped by site (major
607 grouping), collection strategy (CTD or *Alvin*, middle grouping), and deployment (minor groups).
608 Only orders reaching at least 2% abundance in at least one sample are shown. Taxonomy follows
609 SILVA conventions (e.g., Oceanospiralles_3).

610

611 Microbial genera typically associated with aerobic CH_4 oxidation and methylotrophy
612 were detected at low relative abundances (<0.5%) but were consistently present across multiple
613 bottom- water samples (Fig. 5). The most abundant methanotroph across the seep sites, IheB2-23
614 (Methylomonadaceae), was particularly prevalent above Santa Monica Mound, with peak
615 abundance observed in the deepest samples from CTD6 (819 m) and along the CTD7 horizontal
616 transect, where WP8 (~72 m down current from the EK80 CH_4 plume at WP6) exhibited the
617 highest relative abundance. Notably, this group was also the most abundant putative

https://doi.org/10.5194/egusphere-2026-4409
Preprint. Discussion started: 30 July 2026
© Author(s) 2026. CC BY 4.0 License.

methanotroph detected throughout the water column, including within the CH_4 minimum zone of CTD8.

Regarding horizontal methanotroph distribution, the 16S rRNA abundance of methanotrophs remained relatively stable across the 400-m transect at Santa Monica Mound, with consistently low but detectable levels across the waypoints. In contrast, along the horizontal transect across Del Mar Seep (CTD3), aerobic methanotrophs were only detected at WP1 (off-seep), potentially indicating a more restricted distribution. Interestingly, the sample with the highest microbial diversity, AD5194-B (CH_4 74 nM), was collected above an active seep habitat at Del Mar Seep, where carbonate rocks and an orange sulfur bacteria mat were observed. The second most diverse assemblage was noted in AD5199-A (CH_4 2.5 x 10^5 nM), which was taken within the Santa Monica Mound CH_4 plume (Fig. 1e). Notably, no methanotrophs were detected in the water overlying Lasuen Knoll based on 16S rRNA gene sequencing. It is possible that methanotrophic taxa were present at levels below the detection limit of the method, particularly because positive CH_4 oxidation was measured across these depths, indicating ongoing microbial activity. This discrepancy likely reflects the limitations of amplicon sequencing in detecting low abundance but metabolically active community members, as transcriptional activity can be disproportionately higher than their representation in the 16S rRNA amplicon pool (Galambos et al., 2019). Alternatively, it is plausible that CH_4 oxidation at Lasuen Knoll is catalyzed by a group not yet recognized as methanotrophic. The radiotracer incubations confirm that methanotrophs were still present and active at Lasuen Knoll but not captured by the sequencing approach used in this study.

https://doi.org/10.5194/egusphere-2026-4409
Preprint. Discussion started: 30 July 2026
© Author(s) 2026. CC BY 4.0 License.

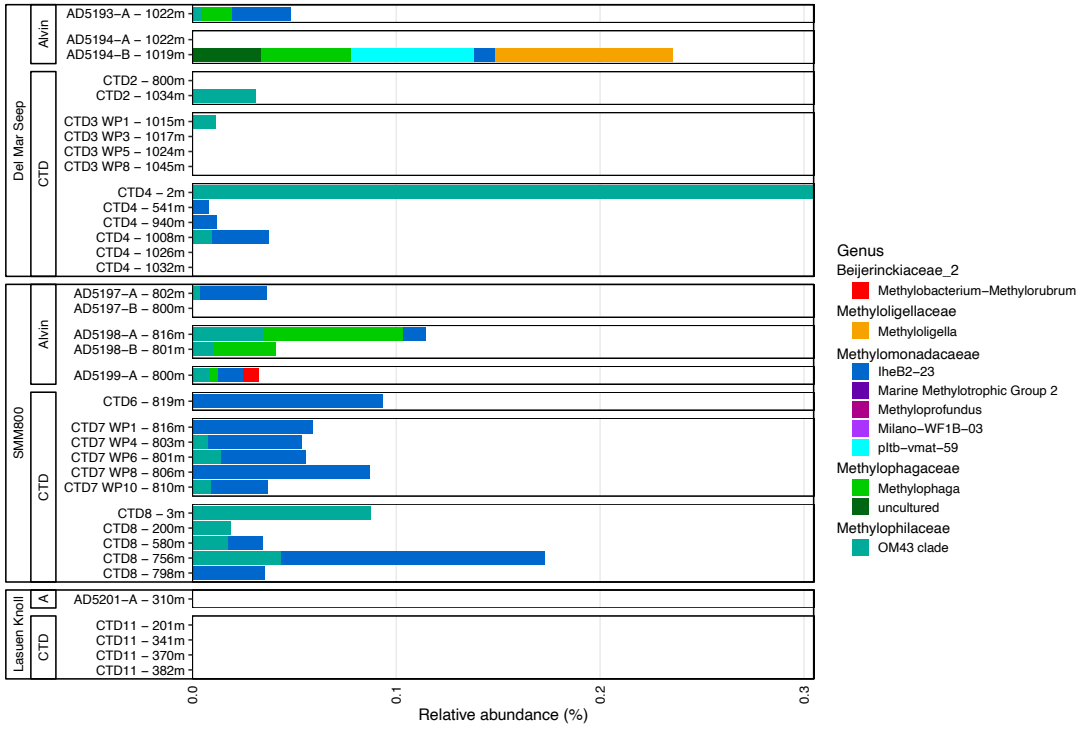

Figure 5. Relative percent abundance of select methanotrophic and methylotrophic genera in samples collected from the water column (CTD and *Alvin* Dives). Relative abundance (x-axis, %) is shown as a stacked bar plot for genera (colored bars) for samples (y-axis) in which this collective of genera reached at least 0.01% abundance. Samples are grouped by site (major grouping), collection strategy (CTD or *Alvin*, middle grouping), and deployment (minor groups). In this figure, all members of Methylomonadaceae are canonical aerobic methanotrophs (Orata et al., 2018). By contrast, *Methylobacterium–Methylorubrum*, *Methyloligella*, the OM43 clade (Methylophilaceae), and most Methylophagaceae (e.g., *Methylophaga*) are methylotrophs; note, however, that some Methylophagaceae lineages in this study possess a divergent *pmoCAB* operon that may confer CH_4-oxidizing potential (Mayr et al., 2025). Although not shown, the related genus *Methyloceanibacter* (Methyloligellaceae) can encode sMMO and behave as a methanotroph (Vekeman et al., 2016).

Quantitative PCR analysis

Vertical CTD casts and *Alvin* Niskin samples at Del Mar Seep, Santa Monica Mound, and Lasuen Knoll revealed strong depth-related patterns in *pmoA* gene abundance, with higher values

https://doi.org/10.5194/egusphere-2026-4409
Preprint. Discussion started: 30 July 2026
© Author(s) 2026. CC BY 4.0 License.

concentrated near deeper seep-influenced waters and lower abundances in midwater and surface layers (Fig. 6 and Table S3). At the Del Mar seep, the highest *pmoA* abundance was detected between 800 and 1,034 m, where values ranged from 5.82 log copies L^{-1} at 800 m to 5.57 log copies L^{-1} at 1,034 m. In contrast, shallower depths displayed lower gene abundance, with 4.65 log copies L^{-1} in the surface water, however, *pmoA* gene abundance remained steady through the CH_4 minima with 5.59 log copies L^{-1} at 540 m. *Alvin* Niskin samples in Del Mar exhibited more pronounced variability, with AD5193-A and AD5194-A yielding moderate values (4.53–4.70 log copies L^{-1}), whereas AD5194-B, while in an active environment, showed a significantly lower abundance of 2.50 log copies L^{-1}, suggesting potential localized differences in methanotrophic community density near active seepage. Santa Monica Mound exhibited a similar depth-related pattern, with *pmoA* values peaking between 752 and 816 m (5.84–6.05 log copies L^{-1}), while surface waters had the lowest abundance (3.49 log copies L^{-1}). In the CH_4 minima, the concentration remained at 5.84 log copies L^{-1}. *Alvin* samples from seep-associated areas showed moderate variability, with AD5198-B recording the highest abundance (5.30 log copies L^{-1}), while AD5198-A (4.77 log copies L^{-1}) and AD5197-B (4.42 log copies L^{-1}) were slightly lower, potentially reflecting differences in seep intensity or population drift from bottom currents. At Lasuen Knoll, *pmoA* abundance ranged from 5.12 to 5.32 log copies L^{-1}, with the highest value recorded at 341 m (5.32 log copies L^{-1}) above the seep and the lowest off-seep at 310 m (AD5201-A; 4.99 log copies L^{-1}). Although no DNA samples were taken in the surface water at Lasuen Knoll, *pmoA* data suggests that the MOB population is distributed throughout the majority of the water column similar to Del Mar Seep and Santa Monica Mound, with moderate *pmoA* abundance at midwater and near the seafloor.

Horizontal CTD transects across the Del Mar Seep and Santa Monica Mound highlight the ubiquity of pmoA in microbial communities over distances likely up to hundreds of meters from active seepage (Fig. 6). Along the Del Mar transect (water depths between 1,015 and 1,045 m), *pmoA* gene abundance remained relatively consistent over short distances, with WP1 and WP3 (~150 m apart) containing similar values of 5.25 and 5.46 log copies L^{-1}, respectively. At WP5, ~150 m from WP3, *pmoA* abundance was stable at 5.45 log copies L^{-1}. At WP8 (~1988 m from WP5), *pmoA* gene abundance remained stable at 5.29 log copies L^{-1}. Given the narrow range observed across sites and the potential limits of detection sensitivity, this suggests minimal variation in methanotroph abundance across this portion of the transect. At Santa Monica Mound

https://doi.org/10.5194/egusphere-2026-4409
Preprint. Discussion started: 30 July 2026
© Author(s) 2026. CC BY 4.0 License.

(water depth between 801 to 816 m), horizontal variability in *pmoA* gene abundance was similarly minimal over short distances and exhibited slight fluctuations across the broader seep field. At WP1 (816 m depth) *pmoA* concentration was 5.88 log copies L^{-1} and at WP4 (~142 m apart) the *pmoA* concentration slightly increased to 6.05 log copies L^{-1}, the highest recorded at this site. WP6, the location of the vigorous CH_4 bubble plume in the EK80, reached a *pmoA* gene abundance of 5.91 log copies L^{-1}. WP8 (~52 m from WP6) retained similarly high values (5.93 log copies L^{-1}). These findings suggest that methanotrophic community concentration remains relatively consistent across short distances (≤100 m), with periphery stations such as WP1 at Del Mar (CTD3), WP1 at Santa Monica Mound (CTD7), and the off-seep CTD6 site at Santa Monica showing similar *pmoA* abundance to nearby on-seep locations. Slight increases in gene copy number were observed in areas of higher CH_4 bubble release, such as WP6 and WP8. Collectively, the vertical and horizontal distributions of *pmoA* gene abundance suggest that the MOB population is highest in deeper waters near active seeps and remains relatively stable over short horizontal distances (≤100 m), while exhibiting some variation across larger spatial scales. A horizontal CTD transect was not conducted for Lasuen Knoll.

https://doi.org/10.5194/egusphere-2026-4409
Preprint. Discussion started: 30 July 2026
© Author(s) 2026. CC BY 4.0 License.

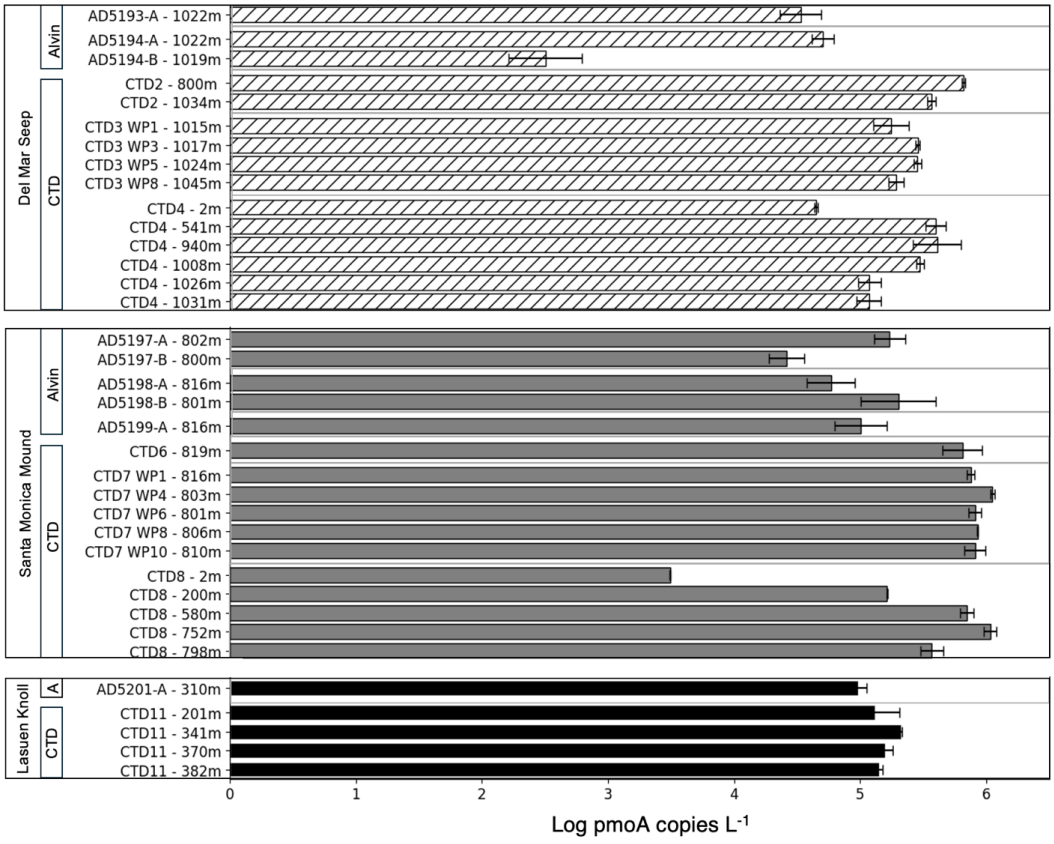

Figure 6. Log-transformed qPCR-derived concentrations of the particulate methane monooxygenase gene (pmoA) in water samples collected at Del Mar Seep (striped bars), Santa Monica Mound (gray bars), and Lasuen Knoll (black bars). Each horizontal bar represents the $\log_{10}$ pmoA copy number per liter for a given sample (labeled by depth, Waypoint (WP), or *Alvin* cast), illustrating the distribution of CH_4-oxidizing microbial populations across depths and seep sites in the Southern California margin. Samples are grouped by site (major grouping), collection strategy (CTD or *Alvin* (A), middle grouping), and deployment (minor groups). Error bars represent the standard deviation.

https://doi.org/10.5194/egusphere-2026-4409
Preprint. Discussion started: 30 July 2026
© Author(s) 2026. CC BY 4.0 License.

4 Discussion

CH_4 and methanotroph transport beyond the seep

Our observations indicate it is possible that both CH_4 and methanotrophs are transported vertically beyond visibly active seep areas (>200 m). Vertical transport within the water column could be conducted via gas bubbles (Jordan et al., 2019; Jordan et al., 2020) and other physical processes including turbulent mixing and seasonal upwelling (Hickey, 1992; Leifer et al., 2006; Pohlman et al., 2017). Alternatively, the planktonic methanotrophic signatures detected on the periphery of the seep may be associated with a rare biosphere in the water column. Elevated CH_4 oxidation rates were consistently detected 10–30 m above the seafloor across the three seep sites (Fig. 2m-p) paired with slight increases (~0.5 log) in *pmoA* gene copy numbers. Most evidently, the EK80 bubble plume at Santa Monica Mound extended vertically from the seafloor to approximately 400 m above the seafloor, which aligned with the CH_4 concentration profile shown in Fig. 2k and CH_4 oxidation in Fig. 2o. It remains unclear whether methanotrophs residing near the seafloor influence microbial community composition in the overlying water column at these sites. However, *pmoA* gene copy numbers remained relatively stable from the bottom waters up to 200 m depth at both Del Mar Seep and Santa Monica Mound.

Horizontal transects revealed spatial patterns in CH_4 oxidation that suggest physical transport influences methanotroph distribution across single seep systems. At Del Mar Seep, average CH_4 oxidation rates increased from WP10 toward WP1, with intermediate values near active seepage sites such as WP3 and WP8. This pattern may reflect redistribution of CH_4 and methanotrophs by a bottom current flowing northwest along the transect, which generally aligns with mean circulation pattern in the Southern California Bight (Hickey, 1992). A similar oxidation gradient was observed at Santa Monica Mound, where rates increased from WP1 to WP10, consistent with a westward current inferred from CH_4 plume morphology. Previous work at this site reported relatively uniform abundances and expression of methanotroph-associated pmoA genes across a transect extending 265 m from the mound despite large differences in CH_4 concentrations (Ussler III et al., 2013). Although CH_4 concentrations were more variable due to localized seepage at Santa Monica Mound, the directional oxidation signal was maintained in this study.

At Haakon Mosby Mud Volcano, low water column CH_4 oxidation rates were attributed to strong bottom currents that displaced CH_4 before microbial communities could respond

https://doi.org/10.5194/egusphere-2026-4409
Preprint. Discussion started: 30 July 2026
© Author(s) 2026. CC BY 4.0 License.

(Sauter et al., 2006). As currents also impact CH_4 release and vary on an hourly time scale from tides and passing eddies (Ussler III et al., 2013), it is difficult to constrain comprehensive CH_4 oxidation without time series sampling. To this point, Ussler et al., 2013 monitored CH_4 concentrations over a seep on the Santa Monica Mound using an in situ mass spectrometer, recording values ranging from 10µM to over 100µM over a 13h period. A similar mechanism may explain elevated CH_4 oxidation at peripheral stations such as WP1 at Del Mar and WP10 at Santa Monica, where CH_4 and methanotrophs appear to be distributed laterally from active seeps. On broader scales, circulation-driven dilution and water mass mixing can suppress oxidation by altering CH_4 availability and methanotroph standing stocks, as shown in Arctic shelf systems (Steinle et al., 2015). In the Santa Barbara Basin, an enclosed system similar to the Santa Monica Basin, episodic bottom water renewal due to springtime upwelling disrupts persistent low-O_2 conditions, with consequences for CH_4 retention and aerobic microbial activity (Qin et al., 2022). Collectively, these transport processes modulate methanotroph dispersal and CH_4 oxidation, expanding the footprint of the methanosphere beyond active seep zones.

Inter- and intra-seep heterogeneity of CH_4, CH_4 oxidation, and community composition

CH_4 seep environments in the Southern California Borderland exhibited pronounced spatial heterogeneity, both within individual seeps and across sites. At Del Mar Seep (~1020 m), low-O_2 bottom waters (min 9.2 µM) coincided with moderate CH_4 concentrations (74–190 nM) and oxidation rates (0.31–0.64 nmol L^{-1} d^{-1}). These conditions, coupled with variable faunal and mat cover, suggest a dynamic environment potentially shaped by organic matter input and limited bottom-water ventilation which impact O_2 concentrations. In contrast, Santa Monica Mound (~800 m) exhibited vigorous CH_4 bubbling, plume formation, and lower bottom water O_2 (~3–4 µM), alongside elevated CH_4 concentrations and oxidation rates (up to 2.61 nmol L^{-1} d^{-1} near the mound, and 454 nmol L^{-1} d^{-1} within the bubble plume). The semi-enclosed hydrography of the Santa Monica Basin may promote CH_4 retention and shape the vertical structure and persistence of methanotrophic communities in the overlying water column. These site-level contrasts support previous findings that circulation patterns and O_2 concentrations modulate CH_4 transport and oxidation efficiency (Hein et al., 2006; Heintz et al., 2012; Paull et al., 2008; Steinle et al., 2015), expanding the functional extent of CH_4 cycling without necessarily altering the underlying seepage dynamics.

https://doi.org/10.5194/egusphere-2026-4409
Preprint. Discussion started: 30 July 2026
© Author(s) 2026. CC BY 4.0 License.

At the Lasuen Knoll site (~310 m), located along an active tectonic structure, *Alvin* observations documented recent seafloor disturbance, including slumped sediment and displacement along the knoll's cliff face, consistent with a submarine slide. While no vigorous venting was observed during the dive, partially buried sulfur bacteria mats suggested prior seepage activity. The site's water column CH_4 and CH_4 oxidation profiles were variable by location, and O_2 concentrations were elevated (~30–32 µM) relative to the conditions observed at deeper seep sites. These features may reflect episodic or spatially diffuse seepage, potentially linked to tectonic forcing or slope instability that intermittently opens migration pathways for CH_4. However, during this dive, sampling was not conducted directly above the subsequently identified active seep site. In the areas sampled with *Alvin*, visible signs of seepage were variable or absent, and activity at the time appeared limited, though measurable methanotrophic oxidation suggests recent or low-level CH_4 input to the water column, likely originating from the nearby seep. Additional surveys and time-series observations will be necessary to resolve the temporal variability of CH_4 release and associated microbial responses at this location.

These contrasts, specifically differences in bottom water O_2 concentration, CH_4 availability, and vertical water column structure across seep sites, highlight the role of localized geochemical and physical gradients in shaping the dynamics of CH_4 transport and oxidation in the water column. Such environmental variability also appears to structure methanotrophic communities. For example, deep-water samples at both Del Mar and Santa Monica Mound contained greater methanotrophic diversity and abundance near the seafloor than higher in the water column, while members of the Methylomonadaceae clade IheB2-23 were also detected throughout the water column. These observations underscore how environmental conditions across and within seep sites influence not only the magnitude of CH_4 oxidation but also the stratification and dispersal of key methanotrophic lineages. Beyond microbes, the fauna at these seep sites exhibits high levels of taxonomic (Lee et al., 2025) and trophic (Pereira et al., 2026) heterogeneity, likely also influenced by CH_4 and O_2 availability.

CH_4 oxidation rates in marine water columns span several orders of magnitude, from $<1 \times 10^{-2}$ to $>1 \times 10^{3}$ nmol L^{-1} d^{-1}, with the highest rates measured in active CH_4 plumes and or in hypoxic environments (Mau et al., 2013; Rogener et al., 2021; Steinle et al., 2015; Steinle et al., 2017). CH_4 oxidation rate (4.54×10^{2} nmol L^{-1} d^{-1}) measured at Santa Monica Mound (station AD5199-A) falls among the upper end of values reported for CH_4-enriched marine systems. This

https://doi.org/10.5194/egusphere-2026-4409
Preprint. Discussion started: 30 July 2026
© Author(s) 2026. CC BY 4.0 License.

elevated activity coincided with a vigorous bubble plume and high CH_4 concentrations, in stark contrast to nearby peripheral sites (e.g., AD5197-B), where CH_4 levels and oxidation rates were markedly lower. In contrast, at Del Mar, two visibly active habitats (AD5193-A and AD5193-B) showed notable intra-site differences. AD5193-A exhibited CH_4 concentrations of 190 nM, 4.5 log pmoA copies L^{-1}, and an oxidation rate of 0.31 nmol L^{-1} d^{-1}, while AD5194-B displayed lower CH_4 concentrations (74 nM) and pmoA levels (2.5 log copies L^{-1}) but a higher oxidation rate (0.64 nmol L^{-1} d^{-1}) and greater methanotroph/methylotroph diversity. Molecular analyses further underscore this heterogeneity, revealing distinct microbial assemblages that vary with seep intensity, geochemical gradients, and physical habitat structure. Moreover, small-scale differences in fluid flow and geological heterogeneity create niche environments that drive localized microbial diversification and patchy higher trophic distributions (Cordes et al., 2010; Levin et al., 2003).

CH_4 turnover and environmental controls

To better understand how environmental conditions shape microbial CH_4 oxidation, turnover times were calculated from measured oxidation rate constants across vertical CTD casts and *Alvin*-collected water samples at all three seep sites (Table 3 and Table S2). These depth-resolved estimates provide insight into how CH_4 oxidation responds to vertical gradients in CH_4 concentration, O_2 availability, and proximity to active seepage.

At both Del Mar Seep and Santa Monica Mound, short turnover near the surface and above the seafloor contrasted with much slower turnover at midwater depths, consistent with CH_4-depleted zones where oxidation was limited. The rapid methane turnover in the surface water despite low CH_4 concentrations and high O_2 suggests cryptic CH_4 cycling, potentially linked to the production of methane by phytoplankton (Mao et al., 2024). During the summer sampling period, CH_4 production in surface waters could for example be facilitated by photosynthesis-driven breakdown of dimethylsulfoniopropionate (DMSP) (Damm et al., 2011; Florez-Leiva et al., 2013; Zhang et al., 2023). Turnover above Santa Monica Mound slowed at midwater depths (~10.1 years), consistent with a CH_4 minimum then accelerated again near the seafloor, with turnover times of 0.40 years at CTD8 and 1.47 years at AD5199-A, sampled within the CH_4 plume, where CH_4 peaked (~293 nM) and O_2 was lowest (~3.3 µM). These patterns echo findings from Eckernförde Bay, where CH_4 oxidation was enhanced under low O_2

https://doi.org/10.5194/egusphere-2026-4409
Preprint. Discussion started: 30 July 2026
© Author(s) 2026. CC BY 4.0 License.

but with limited carbon assimilation (Steinle et al., 2017), highlighting the role of both seep-derived and *in situ* CH_4 supply in regulating turnover.

Despite higher O_2 concentrations at the shallower Lasuen Knoll site, oxidation appeared to remain closely tied to CH_4 availability, reinforcing that CH_4 supply, not just O_2 limitation, drives turnover. This aligns with prior studies from the Santa Monica Basin (Heintz et al., 2012; Ward & Kilpatrick, 1993), where short turnover times tracked zones of elevated CH_4 flux. Moreover, small-scale O_2 and CH_4 gradients may generate microsites of high methanotrophic activity, fueling local biomass production and trophic transfer by animals (Thurber et al., 2013). Environmental factors such as temperature (Fuchs et al., 2016), methanotroph abundance (Tavormina et al., 2013), and carbon quality likely further modulate turnover rates, contributing to the spatial heterogeneity of CH_4 oxidation in seep-influenced water columns.

To further identify the environmental factors regulating the CH_4 oxidation rate constant (k) and turnover time, a Spearman Rank Correlation analysis was conducted across the three seep sites (Fig. 7). The analysis incorporated the most complete available environmental data from CTD4, CTD8, and CTD11, including measurements of CH_4, O_2, temperature, fluorescence (as a proxy for primary productivity), and *pmoA* gene concentration (log copies L^{-1}). As CH_4 oxidation characteristically follows first-order kinetics, CH_4 concentration inherently governs the reaction rate. However, variability in the rate constant (k) reflects differences in how efficiently methanotrophic communities can convert available CH_4 under prevailing environmental conditions. This efficiency is shaped by factors such as approximate MOB abundance (pmoA), O_2 availability, and potentially organic carbon export from the surface ocean as an indirect factor. Therefore, observed differences in k across sites reflect broader ecological and geochemical constraints on CH_4 oxidation.

At Del Mar Seep (Fig. 7a), k displayed only moderate correlations with environmental variables, despite measurable CH_4 concentrations. Although a positive correlation with CH_4 (ρ = 0.49) is expected from first-order kinetics, the weak association between k and pmoA, and the negative correlation with O_2, suggest that physical processes like mixing or seep patchiness may limit the extent to which CH_4 availability translates into active oxidation. The modest positive correlation between fluorescence and k (ρ = 0.26) implies a potential indirect link between surface productivity and methanotrophic activity, but the overall pattern indicates that oxidation

https://doi.org/10.5194/egusphere-2026-4409
Preprint. Discussion started: 30 July 2026
© Author(s) 2026. CC BY 4.0 License.

is not tightly coupled to any single environmental driver. These results highlight that CH_4 presence alone is not sufficient to ensure high oxidation rates.

At Santa Monica Mound (Fig. 7b), *k* showed strong positive correlations with CH_4 (ρ = 0.90), pmoA (ρ = 0.70), and fluorescence (ρ = 0.80), suggesting a system where CH_4 availability, approximate MOB abundance, and surface productivity are all elevated and co-aligned. The strong negative correlation with O_2 (ρ = –0.70) is consistent with enhanced oxidation under low-O_2 conditions, as expected within the Santa Monica Basin OMZ where bottom-water O_2 concentrations fall below 3 µM. Turnover time was inversely correlated with both CH_4 and pmoA, indicating that areas of high CH_4 supply and methanotroph presence correspond to faster CH_4 turnover. Together, these patterns reflect a well-integrated seep system with high CH_4 oxidation capacity.

At Lasuen Knoll (Fig. 7c), k was strongly correlated with CH_4 (ρ = 1.00) and O_2 (ρ = 0.80), and moderately with pmoA (ρ = 0.60), suggesting that CH_4 oxidation here is more O_2-dependent than at the other sites. Located at shallower depth (~450 m), this site lies above the OMZ and experiences higher baseline O_2 availability. The positive correlation with O_2 implies that aerobic CH_4 oxidation is not O_2-limited and may be enhanced under these conditions. Fluorescence was only weakly associated with *k*, suggesting surface productivity plays a minimal role in regulating methanotrophy here. Turnover time correlations were generally weaker, possibly reflecting the influence of variable seepage intensity or recent slope disturbance.

https://doi.org/10.5194/egusphere-2026-4409
Preprint. Discussion started: 30 July 2026
© Author(s) 2026. CC BY 4.0 License.

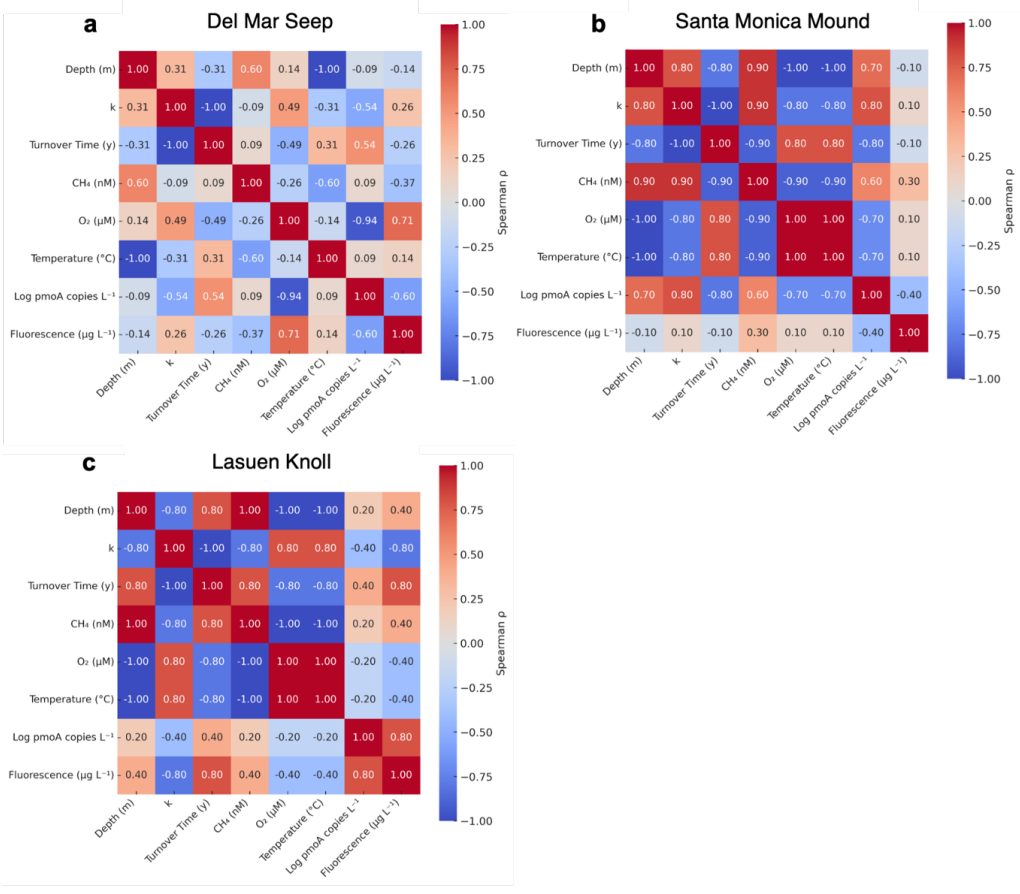

Figure 7. Spearman correlation heatmaps showing relationships among environmental and chemical variables at three CH_4 seep sites: (**a**) Del Mar Seep, (**b**) Santa Monica Mound, and (**c**) Lasuen Knoll. Correlation matrices include depth, CH_4 oxidation rate constant (k), turnover time, methane (CH_4), oxygen (O_2), temperature, pmoA gene concentration (log copies L^{-1}), and fluorescence (proxy for primary productivity). Warmer colors (red) represent stronger positive correlations, while cooler colors (blue) represent stronger negative correlations. Note that Spearman's rank correlation detects monotonic associations but does not imply causality and may be sensitive to outliers or small sample sizes.

https://doi.org/10.5194/egusphere-2026-4409
Preprint. Discussion started: 30 July 2026
© Author(s) 2026. CC BY 4.0 License.

Ecological significance of the methanosphere

Our results provide new insight into the spatial extent and ecological significance of the methanosphere, which encompasses both discrete seep features and the surrounding water column where CH_4 oxidation and MOB may extend beyond the immediate seep environment. As discussed, the transect data from Del Mar Seep and Santa Monica Mound (Fig. 3) show measurable CH_4 oxidation rates extending over several hundred meters from the seep source, with positive rates observed potentially up to 1 km away (Del Mar Seep). The directional CH_4 transport observed at Santa Monica Mound, combined with oxidation activity across the transect, supports the view that the methanosphere is not a static feature but a dynamic microbial envelope shaped by physical circulation and spatial biogeochemical gradients operating in four dimensions, with time as the fourth dimension.

Elevated *pmoA* gene concentrations in the water column, particularly at Santa Monica Mound, indicate that MOB are distributed at least hundreds of meters beyond the immediate seep environment, consistent with diffuse CH_4 enrichment and favorable O_2 conditions. These observations are consistent with prior work showing that aerobic methanotrophs can persist in CH_4-enriched waters removed from direct benthic sources (Steinle et al., 2015) and that their abundance can respond dynamically to CH_4 gradients (Tavormina et al., 2013). Collectively, these findings support an expanded view of the methanosphere as a spatially diffuse, responsive microbial system that contributes significantly to CH_4 turnover in the water column and may influence adjacent biogeochemical regimes (Damm et al., 2010; Reeburgh, 2007).

Although direct measurements of MOB biomass were not made, *pmoA* gene concentrations enable a first-order approximation. Based on published estimates of ~1–2 *pmoA* gene copies per cell (Kolb et al., 2003) and ~10 fg C per cell (Cermak et al., 2017) the observed gene abundances correspond to high nanogram to potentially microgram-scale MOB carbon per liter in some water column samples. Given average bottom current velocities of 5–10 cm s^{-1} in the Santa Monica Basin (Hickey et al., 2003), this suspended microbial biomass could be advected several kilometers per day. Such dispersal may allow methanotrophs to persist in CH_4-poor environments by maintaining low-activity states until CH_4 becomes available, thereby expanding their ecological range and response potential (Reis et al., 2024). Importantly, this advected MOB biomass represents a small but potentially steady microbial carbon source to surrounding heterotrophic food webs. Methanotrophic cells may be consumed by mixotrophic

https://doi.org/10.5194/egusphere-2026-4409
Preprint. Discussion started: 30 July 2026
© Author(s) 2026. CC BY 4.0 License.

protists, suspension feeders, or benthic filter feeders outside active seep zones, linking water column CH_4 oxidation to broader trophic and carbon cycling processes (Boetius & Wenzhöfer, 2013; de Angelis & Lee, 1994; Pernthaler, 2005). This ecological connectivity through consumption is further supported by concurrent observations from the same sites, where macrofaunal communities rapidly reorganized in response to changes in seepage intensity and oxygen availability, transitioning toward non-seep assemblages as CH_4 supply declined (Lee et al., 2025). These patterns likely create spatial gradients in food availability, forming an ecological 'chemotone'- a chemically structured ecological transition zone described by Ashford et al., 2021. The transport of CH_4 off seep could help explain the finding that 62% of the taxa on seep rocks from Mound 12 Costa Rica were able to survive for 17 months after transplantation to an off-seep site (Pereira et al., 2021). Collectively, these results suggest that the methanosphere functions not only as a water column CH_4 sink but also as a vector of microbial biomass, linking seep-associated production to adjacent ecosystems and supporting broader ecological connectivity.

Surface water CH_4 oxidation and implications for cryptic CH_4 cycling

While not as pronounced as the CH_4 oxidation rates near the seafloor, our results reveal active methanotrophy in surface waters despite relatively low CH_4 concentrations. Quantitative PCR analyses confirmed the presence of aerobic methanotrophs in these waters; however, none were identified through 16S sequencing. Methanotrophy may be stimulated by organic precursors like DMSP released during periods of elevated primary productivity (Damm et al., 2010; Karl et al., 2008; Klintzsch et al., 2019). Specifically, during a summer phytoplankton bloom in the Artic Shelf, an *in situ* cycle of CH_4 production and consumption was observed, and an inverse correlation between DMSP and CH_4 suggested that DMSP might serve as a potential substrate for methylotrophic methanogenesis in surface waters (Damm et al., 2010). The enrichment of cyanobacterial taxa (e.g., Synechococcales) in our surface CTD samples further supports the idea that phytoplankton-derived substrates may enhance methanotrophic activity in the upper water column.

Previous studies have shown that while CH_4 concentrations in the surface ocean are typically low, the surface can still act as a significant CH_4 sink, meaning it serves as a net zone of CH_4 removal through rapid microbial oxidation by specialized communities (Hartmann et al.,

https://doi.org/10.5194/egusphere-2026-4409
Preprint. Discussion started: 30 July 2026
© Author(s) 2026. CC BY 4.0 License.

2020). The dynamic spatial and temporal variability of CH_4 in oxic surface waters, combined with rapid microbial turnover times (Table 3), suggests that these environments are more biogeochemically active than traditionally assumed. CH_4 oxidation in surface waters likely responds to CH_4 produced from different pathways linked to phytoplankton productivity (Mao et al., 2024; Perez-Coronel & Michael Beman, 2022). This CH_4 may be rapidly oxidized *in situ* by aerobic methanotrophs, consistent with previously described cryptic CH_4 cycling (Krause & Treude, 2021; Xiao et al., 2017; Xiao et al., 2018). Our findings suggest that surface methanotrophy not only contributes to the biological CH_4 filter but may also support the persistence and dispersal of methanotrophic communities across dynamic oceanic habitats. These insights are important for predicting how future shifts in oceanographic conditions may alter CH_4 cycling and ecosystem function, with implications for both regional biogeochemistry and global carbon budgets.

5 Conclusions

Our study refines the concept of the methanosphere by demonstrating that aerobic CH_4 oxidation and MOB in the water column extend hundreds of meters or more beyond the boundaries of visibly active seepage, with important implications for the fate and footprint of CH_4 in the ocean. Across three distinct seep environments, Santa Monica Mound, Del Mar Seep, and Lasuen Knoll, we observed elevated *pmoA* gene concentrations, CH_4 oxidation activity potentially from seep sources over 1 km away, and directional CH_4 transport through vertical and horizontal processes (e.g., bubble-mediated, bottom currents). These patterns suggest that the methanosphere is not a fixed or localized zone, but a spatially distributed and environmentally responsive microbial system shaped by CH_4 availability, physical transport, and O_2 gradients in the water column.

Site-specific analyses revealed that the drivers of CH_4 oxidation vary depending on local environmental conditions. At Santa Monica Mound, high CH_4 flux, low O_2 concentrations, and elevated MOB abundance support tightly coupled and efficient CH_4 oxidation. In contrast, Del Mar Seep shows weaker coupling between CH_4 and MOB activity, likely due to more variable mixing and higher background O_2 levels. At Lasuen Knoll, a positive correlation between CH_4 oxidation and O_2 points to O_2 availability as a key control, possibly influenced by its shallower depth and episodic fluid flow. Despite these differences, Del Mar Seep and Santa Monica Mound

https://doi.org/10.5194/egusphere-2026-4409
Preprint. Discussion started: 30 July 2026
© Author(s) 2026. CC BY 4.0 License.

exhibit evidence of MOB biomass extending horizontally beyond seep boundaries, suggesting a broader ecological footprint for these communities.

Importantly, the methanosphere functions as a vector for microbial biomass and CH_4-derived carbon export. First-order estimates based on *pmoA* concentrations and regional current velocities indicate that MOB carbon might possibly be transported several kilometers per day. This advected biomass may support heterotrophic food webs outside of seep zones, linking CH_4 oxidation to broader ecological processes. In this way, the methanosphere serves not only as a CH_4 sink, but also as a microbial and biogeochemical interface between seeps and surrounding ecosystems. In a warming ocean, with regions characterized by lower O_2 levels and higher CH_4 concentrations, the adaptive capacity of methanotrophic communities may still support CH_4 oxidation, including in sites with low ambient CH_4, and can seed new habitats with CH_4-oxidizing communities. This extended methanosphere likely plays a critical role in regulating CH_4 budgets in marine ecosystems, with significant implications for regional carbon cycling and broader climate feedback. As ocean conditions continue to change, understanding the integration of microscale and macroscale processes will be essential for predicting how these ecosystems respond and adapt to shifting biogeochemical regimes.

6 Code and Data Availability

Raw reads are available on NCBI SRA under BioProject PRJNA1479037 at accessions SRR39191919-SRR39191890. 16S rRNA processing code via DADA2 is provided in the supplementary material. Water column methane, methane oxidation, and pmoA gene copies data are available from the Biological and Chemical Oceanography Data Management Office (BCO-DMO) at DOI: 10.26008/1912/bco-dmo.986866.1

7 Author Contribution

Emily Klonicki-Ference: Conceptualization (lead), Investigation (lead), Data curation (lead), Formal analysis (lead), Visualization (lead), Writing – original draft (lead), Writing – review and editing (equal). Daniel R. Utter: Software (lead), Formal analysis (supporting), Investigation (supporting), Data curation (supporting), Visualization (supporting), Writing – original draft (supporting), Writing – review and editing (equal). Kira Homola: Investigation (supporting), Visualization (supporting), Data curation (supporting), Writing – review and editing (equal).

https://doi.org/10.5194/egusphere-2026-4409
Preprint. Discussion started: 30 July 2026
© Author(s) 2026. CC BY 4.0 License.

John S. Magyar: Investigation (supporting), Formal analysis (supporting), Writing – review and editing (equal). Victoria J. Orphan: Conceptualization (supporting), Resources (supporting), Supervision (supporting), Funding acquisition (supporting), Investigation (supporting), Formal analysis (supporting), Writing – review and editing (equal). David W. Caress: Software (supporting), Visualization (supporting), Writing – review and editing (equal). Jennifer B. Paduan: Resources (supporting), Visualization (supporting), Writing – review and editing (equal). Lisa Levin: Funding acquisition (lead), Conceptualization (supporting), Supervision (supporting), Resources (supporting), Investigation (supporting), Writing – review and editing (equal). Tina Treude: Conceptualization (lead), Methodology (lead), Project administration (lead), Supervision (lead), Funding acquisition (supporting), Investigation (supporting), Resources (supporting), Writing – review and editing (equal).

8 Competing Interests

The authors declare that they have no known competing financial interests or personal relationships that could have appeared to influence the work reported in this paper. One (or more) of the co-authors is a member of the editorial board of Biogeosciences. In accordance with the journal's editorial policies, the editorial board member(s) had no involvement in the editorial handling or peer-review of this manuscript.

9 Funding

This project was supported by the U.S. National Science Foundation (Award Nos. 2048597 to T.T., 2048720 to L.A.L., 2048666 to V.J.O., 2205998 to K.H., and 2126631 to D.U.).

10 Acknowledgements

We thank UNOLS, the captain and crew of the *R/V Atlantis*, the *Alvin* operations team, the Shipboard Scientific Services Group (SSSGs), and the supporting personnel from the Woods Hole Oceanographic Institution (WHOI) for their outstanding support during the AT50-12 cruise. Their expertise and dedication were essential to the success of this research. We are also thankful to Y. Li for her assistance with night operations and water filtration. We also gratefully acknowledge S. Connon at the California Institute of Technology for her invaluable guidance in

https://doi.org/10.5194/egusphere-2026-4409
Preprint. Discussion started: 30 July 2026
© Author(s) 2026. CC BY 4.0 License.

microbial sample processing. Artificial intelligence tools were used to assist with refining coding for figure and graph development and to support minor grammatical editing and word count reduction.

11 References

Ashford, Oliver S., et al. "A chemosynthetic ecotone—"chemotone"—in the sediments surrounding deep-sea methane seeps." *Limnology and Oceanography* 66.5 (2021): 1687-1702.

Boetius, A., & Wenzhöfer, F. (2013). Seafloor oxygen consumption fuelled by methane from cold seeps. *Nature Geoscience*, *6*(9), 725-734.

Bussmann, I., Matousu, A., Osudar, R., & Mau, S. (2015). Assessment of the radio 3H-CH4 tracer technique to measure aerobic methane oxidation in the water column. *Limnology and Oceanography: Methods*, *13*(6), 312-327.

Callahan, B. J., McMurdie, P. J., Rosen, M. J., Han, A. W., Johnson, A. J. A., & Holmes, S. P. (2016). DADA2: High-resolution sample inference from Illumina amplicon data. *Nature methods*, *13*(7), 581-583.

Cavanaugh, C. M. (1983). Symbiotic chemoautotrophic bacteria in marine invertebrates from sulphide-rich habitats. *Nature*, *302*(5903), 58-61.

Cermak, N., Becker, J. W., Knudsen, S. M., Chisholm, S. W., Manalis, S. R., & Polz, M. F. (2017). Direct single-cell biomass estimates for marine bacteria via Archimedes' principle. *The ISME journal*, *11*(3), 825-828.

Childress, J. J., Fisher, C., Brooks, J., Kennicutt, M., Bidigare, R., & Anderson, A. (1986). A methanotrophic marine molluscan (Bivalvia, Mytilidae) symbiosis: mussels fueled by gas. *Science*, *233*(4770), 1306-1308.

Cordes, E. E., Cunha, M. R., Galeron, J., Mora, C., Olu-Le Roy, K., Sibuet, M., Van Gaever, S., Vanreusel, A., & Levin, L. A. (2010). The influence of geological, geochemical, and biogenic habitat heterogeneity on seep biodiversity. *Marine Ecology*, *31*(1), 51-65.

Dal Bó, B., Guo, Y., Mayr, M. J., Pereira, O. S., Levin, L. A., Orphan, V. J., & Goffredi, S. K. (2025). Methane-powered sea spiders: Diverse, epibiotic methanotrophs serve as a source of nutrition for deep-sea methane seep Sericosura. *Proceedings of the National Academy of Sciences*, *122*(26), e2501422122.

https://doi.org/10.5194/egusphere-2026-4409
Preprint. Discussion started: 30 July 2026
© Author(s) 2026. CC BY 4.0 License.

Damm, E., Helmke, E., Thoms, S., Schauer, U., Nöthig, E., Bakker, K., & Kiene, R. (2010). Methane production in aerobic oligotrophic surface water in the central Arctic Ocean. *Biogeosciences*, *7*(3), 1099-1108.

Damm, E., Thoms, S., Kattner, G., Beszczynska-Möller, A., Nöthig, E.M. and Stimac, I., 2011. Coexisting methane and oxygen excesses in nitrate-limited polar water (Fram Strait) during ongoing sea ice melting. Biogeosciences Discussions, 8(3), pp.5179-5195.

de Angelis, M. A., & Lee, C. (1994). Methane production during zooplankton grazing on marine phytoplankton. *Limnology and Oceanography*, *39*(6), 1298-1308.

Dubilier, N., Bergin, C., & Lott, C. (2008). Symbiotic diversity in marine animals: the art of harnessing chemosynthesis. *Nature Reviews Microbiology*, *6*(10), 725-740.

Eitel, E. M., Utter, D., Connon, S., Orphan, V. J., & Murali, R. (2024). CABO-16S: A Combined Archaea, Bacteria, Organelle 16S database for amplicon analysis of prokaryotes and eukaryotes in environmental samples. *bioRxiv*, 2024.2010. 2023.619938.

Fisher, M. A., Normark, W. R., Langenheim, V. E., Calvert, A. J., & Sliter, R. (2004). The offshore Palos Verdes fault zone near san Pedro, southern California. *Bulletin of the Seismological Society of America*, *94*(2), 506-530.

Florez-Leiva, L., Damm, E. and Farías, L., 2013. Methane production induced by dimethylsulfide in surface water of an upwelling ecosystem. Progress in Oceanography, 112, pp.38-48.

Fuchs, A., Lyautey, E., Montuelle, B., & Casper, P. (2016). Effects of increasing temperatures on methane concentrations and methanogenesis during experimental incubation of sediments from oligotrophic and mesotrophic lakes. *Journal of Geophysical Research: Biogeosciences*, *121*(5), 1394-1406.

Galambos, D., Anderson, R. E., Reveillaud, J., & Huber, J. A. (2019). Genome-resolved metagenomics and metatranscriptomics reveal niche differentiation in functionally redundant microbial communities at deep-sea hydrothermal vents. *Environmental Microbiology*, *21*(11), 4395-4410.

Goffredi, S. K., Tilic, E., Mullin, S. W., Dawson, K. S., Keller, A., Lee, R. W., Wu, F., Levin, L. A., Rouse, G. W., & Cordes, E. E. (2020). Methanotrophic bacterial symbionts fuel dense populations of deep-sea feather duster worms (Sabellida, Annelida) and extend the spatial influence of methane seepage. *Science Advances*, *6*(14), eaay8562.

https://doi.org/10.5194/egusphere-2026-4409
Preprint. Discussion started: 30 July 2026
© Author(s) 2026. CC BY 4.0 License.

Grupe, B. M., Krach, M. L., Pasulka, A. L., Maloney, J. M., Levin, L. A., & Frieder, C. A. (2015). Methane seep ecosystem functions and services from a recently discovered southern California seep. *Marine Ecology*, *36*, 91-108.

Hartmann, J. F., Günthel, M., Klintzsch, T., Kirillin, G., Grossart, H.-P., Keppler, F., & Isenbeck-Schröter, M. (2020). High spatiotemporal dynamics of methane production and emission in oxic surface water. *Environmental science & technology*, *54*(3), 1451-1463.

Hein, J. R., Normark, W. R., McIntyre, B. R., Lorenson, T. D., & Powell, C. L. (2006). Methanogenic calcite, 13C-depleted bivalve shells, and gas hydrate from a mud volcano offshore southern California. *Geology*, *34*(2), 109-112.

Heintz, M., Mau, S., & Valentine, D. (2012). Physical control on methanotrophic potential in waters of the Santa Monica Basin, Southern California. *Limnology and Oceanography*, *57*(2), 420-432.

Hickey, B. M. (1992). Circulation over the Santa Monica-San Pedro basin and shelf. *Progress in Oceanography*, *30*(1-4), 37-115.

Hickey, B. M., Dobbins, E., & Allen, S. E. (2003). Local and remote forcing of currents and temperature in the central Southern California Bight. *Journal of Geophysical Research: Oceans*, *108*(C3).

Hinrichs, K.-U., & Boetius, A. (2002). The anaerobic oxidation of methane: new insights in microbial ecology and biogeochemistry. *Ocean margin systems*, 457-477.

Jordan, S., Treude, T., Leifer, I., Schulz-Vogt, H., & Schmale, O. (2019). Bubble Shuttle: A bubble-mediated bentho-pelagic transport mechanism of methanotrophs and a first study at the Coal Oil Point seep field to identify the controlling parameters. EGU General Assembly Conference Abstracts,

Jordan, S. F., Treude, T., Leifer, I., Janßen, R., Werner, J., Schulz-Vogt, H., & Schmale, O. (2020). Bubble-mediated transport of benthic microorganisms into the water column: Identification of methanotrophs and implication of seepage intensity on transport efficiency. *Scientific reports*, *10*(1), 4682.

Judd, A., & Hovland, M. (2009). *Seabed fluid flow: the impact on geology, biology and the marine environment*. Cambridge University Press.

https://doi.org/10.5194/egusphere-2026-4409
Preprint. Discussion started: 30 July 2026
© Author(s) 2026. CC BY 4.0 License.

Kalyuzhnaya, M., Yang, S., Rozova, O., Smalley, N., Clubb, J., Lamb, A., Gowda, G. N., Raftery, D., Fu, Y., & Bringel, F. (2013). Highly efficient methane biocatalysis revealed in a methanotrophic bacterium. *Nature Communications*, *4*(1), 2785.

Karl, D. M., Beversdorf, L., Björkman, K. M., Church, M. J., Martinez, A., & Delong, E. F. (2008). Aerobic production of methane in the sea. *Nature Geoscience*, *1*(7), 473-478.

Kemnitz, N., Berelson, W. M., Hammond, D. E., Morine, L., Figueroa, M., Lyons, T. W., Scharf, S., Rollins, N., Petsios, E., & Lemieux, S. (2020). Evidence of changes in sedimentation rate and sediment fabric in a low-oxygen setting: Santa Monica Basin, CA. *Biogeosciences*, *17*(8), 2381-2396.

Klintzsch, T., Langer, G., Nehrke, G., Wieland, A., Lenhart, K., & Keppler, F. (2019). Methane production by three widespread marine phytoplankton species: release rates, precursor compounds, and potential relevance for the environment. *Biogeosciences*, *16*(20), 4129-4144.

Knittel, K., & Boetius, A. (2009). Anaerobic oxidation of methane: progress with an unknown process. *Annual review of microbiology*, *63*(1), 311-334.

Kolb, S., Knief, C., Stubner, S., & Conrad, R. (2003). Quantitative detection of methanotrophs in soil by novel pmoA-targeted real-time PCR assays. *Applied and Environmental Microbiology*, *69*(5), 2423-2429.

Krause, S. J., & Treude, T. (2021). Deciphering cryptic methane cycling: Coupling of methylotrophic methanogenesis and anaerobic oxidation of methane in hypersaline coastal wetland sediment. *Geochimica et Cosmochimica Acta*, *302*, 160-174.

Le, J. T., Girguis, P. R., & Levin, L. A. (2022). Using deep-sea images to examine ecosystem services associated with methane seeps. *Marine Environmental Research*, *181*, 105740.

Lee, K. C. (2025). *Macroinvertebrate Communities on Carbonates at Southern California Methane Seeps: Environmental Drivers and Dynamics* UC San Diego].

Lee, K. C., Pereira, O. S., & Levin, L. A. (2025). Environmental drivers and dynamics of macroinvertebrate communities on carbonates at Southern California methane seeps. *Marine Biology Research*, *21*(8-10), 401-416.

Leifer, I., Luyendyk, B. P., Boles, J., & Clark, J. F. (2006). Natural marine seepage blowout: Contribution to atmospheric methane. *Global Biogeochemical Cycles*, *20*(3).

https://doi.org/10.5194/egusphere-2026-4409
Preprint. Discussion started: 30 July 2026
© Author(s) 2026. CC BY 4.0 License.

Levin, L., Girguis, P. R., German, C. R., Brennan, M. L., Tüzün, S., Wagner, J., Smart, C., Kruger, A., Inderbitzen, K., & Le, J. (2016). Exploration and discovery of methane seeps and associated communities in the California Borderland. *Oceanography*, *29*(1), 40-43.

Levin, L. A. (2005). Ecology of cold seep sediments: interactions of fauna with flow, chemistry and microbes. In *Oceanography and Marine Biology* (pp. 11-56). CRC Press.

Levin, L. A., Baco, A. R., Bowden, D. A., Colaco, A., Cordes, E. E., Cunha, M. R., Demopoulos, A. W., Gobin, J., Grupe, B. M., & Le, J. (2016). Hydrothermal vents and methane seeps: rethinking the sphere of influence. *Frontiers in Marine Science*, *3*, 72.

Levin, L. A., Ziebis, W., Mendoza, G. F., Growney, V. A., Tryon, M. D., Brown, K. M., Mahn, C., Gieskes, J. M., & Rathburn, A. E. (2003). Spatial heterogeneity of macrofauna at northern California methane seeps: influence of sulfide concentration and fluid flow. *Marine Ecology Progress Series*, *265*, 123-139.

Liu, J., Zheng, Y., Lin, H., Wang, X., Li, M., Liu, Y., Yu, M., Zhao, M., Pedentchouk, N., & Lea-Smith, D. J. (2019). Proliferation of hydrocarbon-degrading microbes at the bottom of the Mariana Trench. *Microbiome*, *7*, 1-13.

Maloney, J. M., Grupe, B. M., Pasulka, A. L., Dawson, K. S., Case, D. H., Frieder, C. A., Levin, L. A., & Driscoll, N. W. (2015). Transpressional segment boundaries in strike-slip fault systems offshore southern California: implications for fluid expulsion and cold seep habitats. *Geophysical Research Letters*, *42*(10), 4080-4088.

Mao, Y., Lin, T., Li, H., He, R., Ye, K., Yu, W., & He, Q. (2024). Aerobic methane production by phytoplankton as an important methane source of aquatic ecosystems: Reconsidering the global methane budget. *Science of the Total Environment*, *907*, 167864.

Marlow, J. J., Steele, J. A., Ziebis, W., Thurber, A. R., Levin, L. A., & Orphan, V. J. (2014). Carbonate-hosted methanotrophy represents an unrecognized methane sink in the deep sea. *Nature Communications*, *5*(1), 5094.

Martin, M. (2011). Cutadapt removes adapter sequences from high-throughput sequencing reads. *EMBnet. journal*, *17*(1), 10-12.

Mau, S., Blees, J., Helmke, E., Niemann, H., & Damm, E. (2013). Vertical distribution of methane oxidation and methanotrophic response to elevated methane concentrations in stratified waters of the Arctic fjord Storfjorden (Svalbard, Norway). *Biogeosciences*, *10*(10), 6267-6278.

https://doi.org/10.5194/egusphere-2026-4409
Preprint. Discussion started: 30 July 2026
© Author(s) 2026. CC BY 4.0 License.

Mayr, M. J., Parra, S. A., Connon, S. A., Narayanan, A. K., Murali, R., Cremiere, A., & Orphan, V. J. (2025). Distinct Microbial Communities Within and On Seep Carbonates Support Long-term Anaerobic Oxidation of Methane and Novel pMMO Diversity. *bioRxiv*, 2025.2002. 2004.636526.

Muyzer, G., De Waal, E. C., & Uitterlinden, A. (1993). Profiling of complex microbial populations by denaturing gradient gel electrophoresis analysis of polymerase chain reaction-amplified genes coding for 16S rRNA. *Applied and Environmental Microbiology*, *59*(3), 695-700.

Niemann, H., Steinle, L., Blees, J., Bussmann, I., Treude, T., Krause, S., Elvert, M., & Lehmann, M. F. (2015). Toxic effects of lab-grade butyl rubber stoppers on aerobic methane oxidation. *Limnology and Oceanography: Methods*, *13*(1), 40-52.

Orata, F. D., Meier-Kolthoff, J. P., Sauvageau, D., & Stein, L. Y. (2018). Phylogenomic analysis of the gammaproteobacterial methanotrophs (order Methylococcales) calls for the reclassification of members at the genus and species levels. *Frontiers in Microbiology*, *9*, 3162.

Parada, A. E., Needham, D. M., & Fuhrman, J. A. (2016). Every base matters: assessing small subunit rRNA primers for marine microbiomes with mock communities, time series and global field samples. *Environmental Microbiology*, *18*(5), 1403-1414.

Pasulka, A. L., Goffredi, S. K., Tavormina, P. L., Dawson, K. S., Levin, L. A., Rouse, G. W., & Orphan, V. J. (2017). Colonial tube-dwelling ciliates influence methane cycling and microbial diversity within methane seep ecosystems. *Frontiers in Marine Science*, *3*, 276.

Paull, C. K., Hecker, B., Commeau, R., Freeman-Lynde, R., Neumann, C., Corso, W., Golubic, S., Hook, J., Sikes, E., & Curray, J. (1984). Biological communities at the Florida Escarpment resemble hydrothermal vent taxa. *Science*, *226*(4677), 965-967.

Paull, C. K., Normark, W. R., Ussler III, W., Caress, D. W., & Keaten, R. (2008). Association among active seafloor deformation, mound formation, and gas hydrate growth and accumulation within the seafloor of the Santa Monica Basin, offshore California. *Marine Geology*, *250*(3-4), 258-275.

Pereira, O. S., Gonzalez, J., Mendoza, G. F., Le, J., Coscino, C. L., Lee, R. W., Cortés, J., Cordes, E. E., & Levin, L. A. (2021). The dynamic influence of methane seepage on macrofauna inhabiting authigenic carbonates. *Ecosphere*, *12*(10), e03744.

https://doi.org/10.5194/egusphere-2026-4409
Preprint. Discussion started: 30 July 2026
© Author(s) 2026. CC BY 4.0 License.

Pereira, O. S., Survilas, R., Bravo, M. E., & Levin, L. A. (2026). Hard Rock Buffet: Chemosynthetic Carbon Use and Environmental Trophic Structuring of Carbonate-Associated Macrofauna at Southern California Methane Seeps. *Marine Ecology*, *47*(2), e70088.

Perez-Coronel, E., & Michael Beman, J. (2022). Multiple sources of aerobic methane production in aquatic ecosystems include bacterial photosynthesis. *Nature communications*, *13*(1), 6454.

Pernthaler, J. (2005). Predation on prokaryotes in the water column and its ecological implications. *Nature Reviews Microbiology*, *3*(7), 537-546.

Pohlman, J. W., Greinert, J., Ruppel, C., Silyakova, A., Vielstädte, L., Casso, M., Mienert, J., & Bünz, S. (2017). Enhanced CO2 uptake at a shallow Arctic Ocean seep field overwhelms the positive warming potential of emitted methane. *Proceedings of the National Academy of Sciences*, *114*(21), 5355-5360.

Pontiller, B., Martínez-García, S., Joglar, V., Amnebrink, D., Pérez-Martínez, C., González, J. M., Lundin, D., Fernández, E., Teira, E., & Pinhassi, J. (2022). Rapid bacterioplankton transcription cascades regulate organic matter utilization during phytoplankton bloom progression in a coastal upwelling system. *The ISME journal*, *16*(10), 2360-2372.

Qin, Q., Kinnaman, F. S., Gosselin, K. M., Liu, N., Treude, T., & Valentine, D. L. (2022). Seasonality of water column methane oxidation and deoxygenation in a dynamic marine environment. *Geochimica et Cosmochimica Acta*, *336*, 219-230.

Reeburgh, W. S. (2007). Oceanic methane biogeochemistry. *Chemical reviews*, *107*(2), 486-513.

Reis, P. C., Tsuji, J. M., Weiblen, C., Schiff, S. L., Scott, M., Stein, L. Y., & Neufeld, J. D. (2024). Enigmatic persistence of aerobic methanotrophs in oxygen-limiting freshwater habitats. *The ISME journal*, *18*(1), wrae041.

Rogener, M. K., Hunter, K. S., Rabalais, N. N., Roberts, B. J., Bracco, A., Stewart, F. J., & Joye, S. B. (2021). Pelagic denitrification and methane oxidation in oxygen-depleted waters of the Louisiana shelf. *Biogeochemistry*, *154*, 231-254.

Rubin-Blum, M., Antony, C. P., Sayavedra, L., Martínez-Pérez, C., Birgel, D., Peckmann, J., Wu, Y.-C., Cardenas, P., MacDonald, I., & Marcon, Y. (2019). Fueled by methane: deep-sea sponges from asphalt seeps gain their nutrition from methane-oxidizing symbionts. *The ISME journal*, *13*(5), 1209-1225.

https://doi.org/10.5194/egusphere-2026-4409
Preprint. Discussion started: 30 July 2026
© Author(s) 2026. CC BY 4.0 License.

Ryan, H. F., Conrad, J. E., Paull, C., & McGann, M. (2012). Slip rate on the San Diego Trough fault zone, Inner California Borderland, and the 1986 Oceanside earthquake swarm revisited. *Bulletin of the Seismological Society of America*, *102*(6), 2300-2312.

Sauter, E. J., Muyakshin, S. I., Charlou, J.-L., Schlüter, M., Boetius, A., Jerosch, K., Damm, E., Foucher, J.-P., & Klages, M. (2006). Methane discharge from a deep-sea submarine mud volcano into the upper water column by gas hydrate-coated methane bubbles. *Earth and Planetary Science Letters*, *243*(3-4), 354-365.

Schmaljohann, R., & Flügel, H. J. (1987). Methane-oxidizing bacteria in Pogonophora. *Sarsia*, *72*(1), 91-98.

Semrau, J. D., DiSpirito, A. A., & Yoon, S. (2010). Methanotrophs and copper. *FEMS microbiology reviews*, *34*(4), 496-531.

Sibuet, M., & Roy, K. O.-L. (2002). Cold seep communities on continental margins: structure and quantitative distribution relative to geological and fluid venting patterns. In *Ocean margin systems* (pp. 235-251). Springer.

Steinle, L., Graves, C. A., Treude, T., Ferré, B., Biastoch, A., Bussmann, I., Berndt, C., Krastel, S., James, R. H., & Behrens, E. (2015). Water column methanotrophy controlled by a rapid oceanographic switch. *Nature Geoscience*, *8*(5), 378-382.

Steinle, L., Maltby, J., Treude, T., Kock, A., Bange, H. W., Engbersen, N., Zopfi, J., Lehmann, M. F., & Niemann, H. (2017). Effects of low oxygen concentrations on aerobic methane oxidation in seasonally hypoxic coastal waters. *Biogeosciences*, *14*(6), 1631-1645.

Suess, E. (2010). Marine cold seeps. In. Springer.

Tavormina, P. L., Ussler III, W., Joye, S. B., Harrison, B. K., & Orphan, V. J. (2010). Distributions of putative aerobic methanotrophs in diverse pelagic marine environments. *The ISME journal*, *4*(5), 700-710.

Tavormina, P. L., Ussler III, W., Steele, J. A., Connon, S. A., Klotz, M. G., & Orphan, V. J. (2013). Abundance and distribution of diverse membrane-bound monooxygenase (C u-MMO) genes within the C osta R ica oxygen minimum zone. *Environmental Microbiology Reports*, *5*(3), 414-423.

Thamdrup, B., Steinsdóttir, H. G., Bertagnolli, A. D., Padilla, C. C., Patin, N. V., Garcia-Robledo, E., Bristow, L. A., & Stewart, F. J. (2019). Anaerobic methane oxidation is an

https://doi.org/10.5194/egusphere-2026-4409
Preprint. Discussion started: 30 July 2026
© Author(s) 2026. CC BY 4.0 License.

important sink for methane in the ocean's largest oxygen minimum zone. *Limnology and Oceanography*, *64*(6), 2569-2585.

Thompson, M., & Francis, R. D. (2019). Tectonic Evolution of the Palos Verdes Fault–Lasuen Knoll Segment, Offshore Southern California.

Thurber, A. R., Levin, L. A., Rowden, A. A., Sommer, S., Linke, P., & Kröger, K. (2013). Microbes, macrofauna, and methane: a novel seep community fueled by aerobic methanotrophy. *Limnology and Oceanography*, *58*(5), 1640-1656.

Thurber, A. R., Sweetman, A. K., Narayanaswamy, B. E., Jones, D. O., Ingels, J., & Hansman, R. (2014). Ecosystem function and services provided by the deep sea. *Biogeosciences*, *11*(14), 3941-3963.

Treude, T., Boetius, A., Knittel, K., Wallmann, K., & Jørgensen, B. B. (2003). Anaerobic oxidation of methane above gas hydrates at Hydrate Ridge, NE Pacific Ocean. *Marine Ecology Progress Series*, *264*, 1-14.

Treude, T., Kiel, S., Linke, P., Peckmann, J., & Goedert, J. L. (2011). Elasmobranch egg capsules associated with modern and ancient cold seeps: a nursery for marine deep-water predators. *Marine Ecology Progress Series*, *437*, 175-181.

Tunnicliffe, V., Juniper, S. K., & Sibuet, M. (2003). Reducing environments of the deep-sea floor. *Ecosystems of the World*, 81-110.

Ussler III, W., Preston, C., Tavormina, P., Pargett, D., Jensen, S., Roman, B., Marin III, R., Shah, S. R., Girguis, P. R., & Birch, J. M. (2013). Autonomous application of quantitative PCR in the deep sea: in situ surveys of aerobic methanotrophs using the deep-sea environmental sample processor. *Environmental science & technology*, *47*(16), 9339-9346.

Vekeman, B., Kerckhof, F. M., Cremers, G., De Vos, P., Vandamme, P., Boon, N., Op den Camp, H. J., & Heylen, K. (2016). New Methyloceanibacter diversity from North Sea sediments includes methanotroph containing solely the soluble methane monooxygenase. *Environmental microbiology*, *18*(12), 4523-4536.

Ward, B., & Kilpatrick, K. (1993). Methane oxidation associated with mid-depth methane maxima in the Southern California Bight. *Continental Shelf Research*, *13*(10), 1111-1122.

https://doi.org/10.5194/egusphere-2026-4409
Preprint. Discussion started: 30 July 2026
© Author(s) 2026. CC BY 4.0 License.

Xiao, K.-Q., Beulig, F., Kjeldsen, K. U., Jørgensen, B. B., & Risgaard-Petersen, N. (2017). Concurrent methane production and oxidation in surface sediment from Aarhus Bay, Denmark. *Frontiers in Microbiology*, *8*, 1198.

Xiao, K. Q., Beulig, F., Røy, H., Jørgensen, B. B., & Risgaard-Petersen, N. (2018). Methylotrophic methanogenesis fuels cryptic methane cycling in marine surface sediment. *Limnology and Oceanography*, *63*(4), 1519-1527.

Yamamoto, S., Alcauskas, J. B., & Crozier, T. E. (1976). Solubility of methane in distilled water and seawater. *Journal of Chemical and Engineering Data*, *21*(1), 78-80.

Zhang, Y., Tan, D.D., He, Z., Yu, J. and Yang, G.P., 2023. Dimethylated sulfur, methane and aerobic methane production in the Yellow Sea and Bohai Sea. *Journal of Geophysical Research: Oceans*, *128*(8), p.e2023JC019736.